

# STLCCP: An Efficient Convex Optimization-based Framework for Signal Temporal Logic Specifications

Yoshinari Takayama, Kazumune Hashimoto, Toshiyuki Ohtsuka

**Abstract**—Signal Temporal Logic (STL) is capable of expressing a broad range of temporal properties that controlled dynamical systems must satisfy. In the literature, both mixed-integer programming (MIP) and nonlinear programming (NLP) methods have been applied to solve optimal control problems with STL specifications. However, neither approach has succeeded in solving problems with complex long-horizon STL specifications within a realistic timeframe. This study proposes a new optimization framework, called *STLCCP*, which explicitly incorporates several structures of STL to mitigate this issue. The core of our framework is a structure-aware decomposition of STL formulas, which converts the original program into a difference of convex (DC) programs. This program is then solved as a convex quadratic program sequentially, based on the convex-concave procedure (CCP). Our numerical experiments on several commonly used benchmarks demonstrate that this framework can effectively handle complex scenarios over long horizons, which have been challenging to address even using state-of-the-art optimization methods.

**Index Terms**—Convex optimization, optimal control, formal methods, signal temporal logic

## I. INTRODUCTION

Autonomous robotic systems, such as self-driving cars, drones, and cyber-physical systems, are expected to have extensive real-world applications in transportation, delivery, and industrial automation in the near future. These systems must perform complex control tasks while ensuring safety, ideally with formal guarantees. In response to this need, researchers have developed formal specification languages that offer a unified and rigorous approach to expressing complex requirements for safe and reliable autonomous systems. One such language is signal temporal logic (STL) [1], which is well-suited for continuous real-valued signals. It offers a useful quantitative semantics called *robustness* [2], which quantifies how robustly a formula is satisfied. By maximizing this score, control input sequences can be synthesized robustly, and the resulting trajectories can formally satisfy the specification. However, precisely formulating this optimization problem as a mixed-integer program (MIP) is known to be problematic in terms of scalability with respect to the length of the horizon.

To avoid this issue, recent work has focused on formulating the problem as nonlinear programs (NLP) by smooth approximations of the max and min operators in the robustness

function [3, 4, 5]. These NLP are then solved *naively* through a sequential quadratic programming (SQP) method (or other gradient-based methods). While these SQP-based methods are generally faster and more scalable than MIP-based methods, their major drawback is that they can easily become infeasible and may not find the global optima due to the iterative approximations. For instance, the traditional SQP method approximates the original problem to a quadratic program, which retains only up to the second derivative information of the original problem. This drawback can become even more pronounced when problem structures are not exploited. Specifically, in control problems with STL specifications, the non-convex robustness function in the cost function is frequently coarsely approximated by the traditional SQP method.

This study aims to tackle these issues by explicitly incorporating several *structures of STL*. To accomplish this, we introduce a novel optimization framework, called *STLCCP*, which uses the convex-concave procedure (CCP) [6, 7] for iterative optimization. The STLCCP framework can handle *any* STL specifications and consists of three steps: the preparation step, the reformulation step, and the solving step (refer to Algorithm 3). In contrast to the conventional SQP method, the proposed framework retains complete information of convex parts at each iteration, resulting in fewer approximations. Furthermore, it is designed to be computationally efficient: when the system satisfies the linearity assumption, it solves quadratic programs sequentially, with only disjunctive parts of the specification being linearized at each iteration. Although our framework can handle the general nonlinear case where it becomes a method that solves non-quadratic convex programs sequentially, in this paper, we focus on the linear case for simplicity. Open-source code is available at <https://github.com/yotakayama/STLCCP>.

### A. Contributions

The contributions of this paper are multi-fold as follows.

- i) To introduce the idea of the CCP for control problems with STL specifications, we propose a new *robustness decomposition* framework, which converts the robustness function into a set of constraints systematically. By considering the structures of STL, this decomposition reduces the non-convex parts of the program and makes the convex parts quadratic (or linear). As a result, *STLCCP* becomes an efficient SQP (CCP-based SQP) method.
- ii) To guide the optimization steps not to neglect the *important* constraints, we improve the CCP-based algorithm further by prioritizing those constraints. This method, termed *tree-weighted penalty CCP (TWP-CCP)*, leverages the hierarchical nature of STL by exploiting the structure of the reformulated program.

Y. Takayama is with University Paris-Saclay, CNRS, CentraleSupélec, Laboratory of Signals and Systems (L2S), Gif-sur-Yvette, France. K. Hashimoto is with the Graduate School of Engineering, Osaka University, Osaka, Japan. T. Ohtsuka is with the Graduate School of Informatics, Kyoto University, Kyoto, Japan. Corresponding author: Yoshinari Takayama. This work was completed when the first author was at Kyoto University. This work was supported in part by JSPS KAKENHI under Grant JP22H01510 and 21K14184 and by JST CREST under Grant JPMJCR201. Email: {yoshinari.takayama@l2s.centralesupelec.fr, hashimoto@eei.eng.osaka-u.ac.jp, ohtsuka@i.kyoto-u.ac.jp}

- iii) We propose a new smooth robustness measure that is suitable for our framework using a novel smoothing function, which we call a *mellowmin* function. This robustness has not only soundness and asymptotic completeness properties, but also the tradeoff between the roughness of the majorization and the completeness of the smooth approximation. Additionally, we propose a warm start approach for the efficient utilization of this measure in practice.
- iv) The results of our numerical experiments on several benchmarks indicate that our proposed method outperforms state-of-the-art methods in terms of both robustness score and computational time.

### B. Key feature of our framework

One of the key features of our framework is its ability to exploit the structures of STL specifications. These structures can be divided into three categories: first, all the logical operators in STL specifications, including temporal operators, can be integrally explained using the terms *conjunctive* or *disjunctive*, corresponding to the max or min functions of robustness function, second, the robustness function has a *monotonicity property*, and third, the logical operators in an STL specification have a *hierarchical tree structure*. In the following, we elaborate on how our framework exploits these three properties:

**Conjunctive-disjunctive to convex-concave:** We formally establish a *correspondence* between conjunctive and disjunctive operators and the convexity or concavity of the optimization program. This allows us to reformulate the problem into a DC program by mapping conjunctive operators to convex parts of the program and disjunctive operators to concave parts (see Section III).

**Monotonicity property:** We utilize the monotonicity property to make the reformulation more rigorous and precise. This precise reformulation of the original problem into a DC program minimizes information loss due to approximations (see Section IV).

**Hierarchical structure:** We exploit the information of *priority ranking* among the constraints to avoid significant violations of important constraints in a hierarchical manner (see Section VI). The literature has not utilized this priority ranking among the nodes although some papers also viewed STL as a tree. This is because the naive formulation makes it difficult to differentiate the importance of each node. However, we overcome this challenge through the reformulation.

In addition to the hierarchical priority structure, the perspective of viewing the robustness function as a tree is important throughout this paper and is utilized in many ways. For instance, we apply the formula simplification technique in [8] to reduce the part that we approximate at each step.

### C. Related works

**Control under temporal logic specifications:** Traditionally, approaches based on the abstraction of models have been effective in solving the trajectory synthesis problem under temporal logic specifications. However, they require a

significant amount of domain expertise that is difficult to be automated. Another class of trajectory synthesis algorithms for this problem is the optimization-based approach. While the early papers [9, 10] consider linear temporal logic (LTL) and metric temporal logic (MTL), recent work considers STL specifications [11, 12] as it is more suited to robotic systems with continuous states. Most of these studies have focused on either developing a new metric of robustness [13, 14] or proposing an efficient technique for a specific class of temporal logic specifications [12]. However, these works did not leverage the structure of STL for optimization algorithms. Although there has been recent research that attempts to exploit the tree structure of STL to enhance MIP-based optimization algorithms, such as [8] which reduces the number of integer variables or [15] which proposes a new encoding method for multi-agent problems, these methods do not aim to improve NLP-based algorithms and do not comprehensively use the structures of STL as in this study.

**Control using convex optimizations:** Convex optimization-based frameworks, such as CCP, have been applied in the field of optimal control in some papers, such as [16, 17]. Recently, these frameworks have also been applied in interdisciplinary research between formal methods and control theory. For example, [18] considered parameter synthesis problems in MDPs, and [19] derived the invariant barrier certificate condition for unbounded time safety. Despite the recent popularity of convex optimization, its application to STL specifications has not yet been explored extensively, although several convex optimization-based frameworks for STL specifications are available, such as [20, 21]. While [20] focuses on the decomposition of global STL specifications assigned to multi-agent systems into local STL tasks, our framework addresses the trajectory synthesis problem for a single system. Additionally, [21] applied a convex optimization-based approach for STL specifications, but their solver had to constrain the updates within a trust region, unlike CCP-based approaches, and their approximated parts are completely different from ours.

Furthermore, there has been no previous work that applies the CCP idea to control problems with STL specifications, except for the conference version of this paper [22], which essentially corresponds to the contribution presented in Subsection I-A (i). However, the robustness decomposition approach presented in this paper is applicable to a wider range of STL specifications than the simple specification considered in [22]. Furthermore, all contributions listed in Subsection I-A (ii) and (iii) are not covered in the conference paper.

### D. Organization of this paper

We first provide the problem statement and the preliminary tools in Sections II and III. Section IV presents our robustness decomposition method that transforms the optimization problem to a non-smoothed DC form. Then, the DC program is smoothed by a new smooth function that fits our convex optimization framework in Section V. Section VI proposes the tree-weight penalty CCP to solve the reformulated DC program. Section VII provides numerical experiments and Section VIII concludes our paper.

## II. PROBLEM STATEMENT

$\mathbb{R}$  and  $\mathbb{Z}$  are defined as the sets of real and integer numbers, respectively. Given  $a, b \in \mathbb{Z}$  with  $a < b$ ,  $[a, b]$  denotes a set of integers from  $a$  to  $b$ . True and false are denoted by  $\top$  and  $\perp$ .  $I_n$  denotes the identity matrix of size  $n$ .  $0_{n \times m}$  denotes the zero matrix of size  $n \times m$ .

### A. System description

In this study, we consider a discrete-time linear system

$$x_{t+1} = Ax_t + Bu_t, \quad (1)$$

where  $A \in \mathbb{R}^{n \times n}$  and  $B \in \mathbb{R}^{n \times m}$  are matrices that represent the dynamics of the system. The state at time  $t$  is denoted by  $x_t \in \mathcal{X} \subseteq \mathbb{R}^n$ , and the input at time  $t$  is denoted by  $u_t \in \mathcal{U} \subseteq \mathbb{R}^m$ . We assume that both the state and input sets,  $\mathcal{X}$  and  $\mathcal{U}$ , respectively, are a conjunction of polyhedra.

*Remark 1:* The linearity assumptions we have made were just for the sake of simplicity. Our approach can be directly applied to nonlinear systems of the form  $x_{t+1} = f(x_t) + g(u_t)$  and nonlinear feasible regions  $\mathcal{U}, \mathcal{X}$  as well if all nonlinear functions in  $\mathcal{U}, \mathcal{X}$ , and  $f, g$  are either convex or concave.

Let  $\mathbf{x} = [x_0, \dots, x_T]^\top$  and  $\mathbf{u} = [u_0, \dots, u_{T-1}]^\top$ . Given an initial state  $x_0 \in \mathcal{X}$  and a sequence of control inputs  $u_0, \dots, u_{T-1}$ , the sequence of states  $x_0, \dots, x_T$ , which we refer to as a *trajectory*, is uniquely generated. We define the trajectory starting at timestep  $t$  as  $(\mathbf{x}, t)$ , i.e.,  $(\mathbf{x}, t) = x_t, x_{t+1}, \dots, x_T$ .

### B. Specification by signal temporal logic

The entire set of STL specifications is taken into account in this study. STL is a predicate logic used to specify continuous signal properties [2]. Predicates  $\mu$  are a part of STL and can be acquired through function  $g^\mu(\mathbf{x})$  in the following manner:

$$\mu = \begin{cases} \top & \text{if } g^\mu(\mathbf{x}) \leq 0 \\ \perp & \text{if } g^\mu(\mathbf{x}) > 0 \end{cases}, \quad (2)$$

where  $g^\mu$  is restricted to an affine function  $g^\mu(x_t) = a^\top x_t - b$ :  $\mathcal{X} \rightarrow \mathbb{R}$ , where  $a \in \mathbb{R}^n$  and  $b \in \mathbb{R}$ . In addition to the standard boolean operators  $\wedge$  and  $\vee$ , the STL also incorporates temporal operators  $\square$  (*always*),  $\diamond$  (*eventually*), and  $\mathbf{U}$  (*until*). It is assumed that formulas are written in negation normal form (NNF) without loss of generality. The negations of STL formulas in NNF are solely present in front of the predicates [23, 24] and negations are omitted from the STL syntax. STL in NNF will simply be referred to as STL in the following. The semantics of STL is defined as follows [25]:

$$\varphi := \mu \mid \varphi \mid \varphi \mid \square_{[t_1, t_2]} \varphi \mid \diamond_{[t_1, t_2]} \varphi \mid \varphi \mathbf{U}_{[t_1, t_2]} \varphi.$$

Each temporal operator has associated bounded time interval  $[t_1, t_2]$  where  $0 \leq t_1 < t_2$  and  $t_2 < \infty$ .

The concept of *robustness* is a significant semantics defined for STL formulas, which is a real-valued function that characterizes how well a trajectory satisfies an STL formula. The original robustness of an STL formula  $\varphi$  with respect to a

trajectory  $\mathbf{x}$  and a time  $t$  can be obtained recursively according to the following quantitative semantics:

$$\begin{aligned} \rho_{\text{orig}}^\mu((\mathbf{x}, t)) &= -g^\mu(x_t) \\ \rho_{\text{orig}}^{\varphi_1 \wedge \varphi_2}((\mathbf{x}, t)) &= \min(\rho_{\text{orig}}^{\varphi_1}((\mathbf{x}, t)), \rho_{\text{orig}}^{\varphi_2}((\mathbf{x}, t))) \\ \rho_{\text{orig}}^{\varphi_1 \vee \varphi_2}((\mathbf{x}, t)) &= \max(\rho_{\text{orig}}^{\varphi_1}((\mathbf{x}, t)), \rho_{\text{orig}}^{\varphi_2}((\mathbf{x}, t))) \\ \rho_{\text{orig}}^{\square_{[t_1, t_2]} \varphi}((\mathbf{x}, t)) &= \min_{t' \in [t+t_1, t+t_2]} (\rho_{\text{orig}}^\varphi((\mathbf{x}, t'))) \\ \rho_{\text{orig}}^{\diamond_{[t_1, t_2]} \varphi}((\mathbf{x}, t)) &= \max_{t' \in [t+t_1, t+t_2]} (\rho_{\text{orig}}^\varphi((\mathbf{x}, t'))) \\ \rho_{\text{orig}}^{\varphi_1 \mathbf{U}_{[t_1, t_2]} \varphi_2}((\mathbf{x}, t)) &= \min_{t' \in [t+t_1, t+t_2]} \left( \max \left( \left[ \rho_{\text{orig}}^{\varphi_1}((\mathbf{x}, t')), \right. \right. \right. \\ &\quad \left. \left. \left. \max_{t'' \in [t+t_1, t']} (\rho_{\text{orig}}^{\varphi_2}((\mathbf{x}, t''))) \right] \right) \right) \end{aligned} \quad (3)$$

We abbreviate  $(\mathbf{x}, 0)$  by  $\mathbf{x}$ . For example,  $(\mathbf{x}, 0) \models \varphi$  is abbreviated as  $\mathbf{x} \models \varphi$ . Note that we define  $\rho_{\text{orig}}^\mu((\mathbf{x}, t)) := -g^\mu(x_t)$  because  $\mathbf{x} \models \mu$  if  $g^\mu(x_0) \leq 0$ . The trajectory length  $T$  has to be chosen so that it is longer than *the formula length* of  $\varphi$ , which is the horizon needed to calculate the robustness of a formula (see e.g. [24] for the recursive calculation of formula lengths). By maximizing the robustness  $\rho_{\text{orig}}^\varphi$  that results from (3), a robust control input sequence can be synthesized. The robustness defined above, which we call *original robustness*, is sound in the sense that

$$\rho_{\text{orig}}^\varphi(\mathbf{x}) \geq 0 \implies \mathbf{x} \models \varphi, \quad (4)$$

and also complete<sup>1</sup> in the sense that

$$\rho_{\text{orig}}^\varphi(\mathbf{x}) < 0 \implies \mathbf{x} \not\models \varphi. \quad (5)$$

These properties can be used to ensure that the trajectory satisfies (or violates) the specifications. Moreover, the robustness value plays a role as an indicator of how much margin we have until the border between satisfaction and violation.

### C. Problem

This study considers the control problem with STL specifications. As cost-minimization formulations are more common in the control community than reward-maximization formulations, this problem can be formulated as follows:

*Problem 1:* Given an initial state  $x_0$  and an STL specification  $\varphi$ , solve the following optimization problem:

$$\min_{\mathbf{x}, \mathbf{u}} -\rho_{\text{orig}}^\varphi(\mathbf{x}) \quad (6a)$$

$$\text{s.t. } x_{t+1} = Ax_t + Bu_t \quad (6b)$$

$$x_t \in \mathcal{X}, u_t \in \mathcal{U} \quad (6c)$$

$$\rho_{\text{orig}}^\varphi(\mathbf{x}) \geq 0 \quad (6d)$$

*Remark 2:* Although we omit the quadratic cost terms in the cost function for simplicity in the following sections, the proposed method is also practically useful even when they are added, which is demonstrated in the numerical experiments.

<sup>1</sup>Throughout this paper, we use *soundness* to describe when a robustness value can guarantee the satisfaction of a formula, as in (4). On the other hand, we use *completeness* to describe when a robustness value can also guarantee the violation of a formula, as in (5). These terminologies are the same as [5] but are different from [13]. See [5] for a similar explanation.

### III. PRELIMINARIES

In this section, we provide tools to discuss our approach. Specifically, we first reverse the robustness definition (Subsection III-A). Then, we define the robustness tree for the reversed robustness in Subsection V-B.

#### A. Robustness flipping

The reversed version of the robustness measure  $\rho_{\text{rev}}$  is defined as follows.

*Definition 1: (Reversed robustness)*

$$\rho_{\text{rev}}^{\mu}((\mathbf{x}, t)) = g^{\mu}(x_t) \quad (7a)$$

$$\rho_{\text{rev}}^{\varphi_1 \wedge \varphi_2}((\mathbf{x}, t)) = \max(\rho_{\text{rev}}^{\varphi_1}((\mathbf{x}, t)), \rho_{\text{rev}}^{\varphi_2}((\mathbf{x}, t))) \quad (7b)$$

$$\rho_{\text{rev}}^{\varphi_1 \vee \varphi_2}((\mathbf{x}, t)) = \min(\rho_{\text{rev}}^{\varphi_1}((\mathbf{x}, t)), \rho_{\text{rev}}^{\varphi_2}((\mathbf{x}, t))) \quad (7c)$$

$$\rho_{\text{rev}}^{\square_{[t_1, t_2]} \varphi}((\mathbf{x}, t)) = \max_{t' \in [t+t_1, t+t_2]} (\rho_{\text{rev}}^{\varphi}((\mathbf{x}, t'))) \quad (7d)$$

$$\rho_{\text{rev}}^{\diamond_{[t_1, t_2]} \varphi}((\mathbf{x}, t)) = \min_{t' \in [t+t_1, t+t_2]} (\rho_{\text{rev}}^{\varphi}((\mathbf{x}, t'))) \quad (7e)$$

$$\rho_{\text{rev}}^{\mathcal{U}_{[t_1, t_2]} \varphi_2}((\mathbf{x}, t)) = \max_{t' \in [t+t_1, t+t_2]} \left( \min(\rho_{\text{rev}}^{\varphi_1}((\mathbf{x}, t')), \right. \quad (7f)$$

$$\left. \min_{t'' \in [t+t_1, t']} (\rho_{\text{rev}}^{\varphi_2}((\mathbf{x}, t'')))) \right) \quad (7g)$$

In the above definition, we reverse the sign of the robustness functions  $\rho_{\text{rev}}^{\mu}$  of predicates  $\mu$  in (7a), and we interchange the max functions and the min functions in (7b)–(7g). The reversed robustness  $\rho_{\text{rev}}$  satisfies the equation

$$\rho_{\text{rev}}^{\varphi} = -\rho_{\text{orig}}^{\varphi}. \quad (8)$$

The rationale for flipping the robustness is to establish a clear relationship between conjunctive operators (resp. disjunctive operators) and convex functions (resp. concave functions), as presented in Table I.

TABLE I: Correspondance in the reversed robustness.

functions	convex/concave	tree node-type	operator
max	convex	conjunctive	$\wedge, \square$
min	concave	disjunctive	$\vee, \diamond$

With this modification, unfavorable minus sign symbols can be removed, and the subsequent section's decomposition procedure can be simplified. For instance, consider a formula  $\varphi = \varphi_1 \wedge \varphi_2$ , where  $\varphi_1$  and  $\varphi_2$  are predicates. When using the original robustness, the cost function  $-\rho_{\text{orig}}^{\varphi}$  in Problem 1 is  $-\min(-g^{\varphi_1}, -g^{\varphi_2})$ . On the other hand, when using the reversed robustness  $\rho_{\text{rev}}^{\varphi}$ , the cost function is  $\max(g^{\varphi_1}, g^{\varphi_2})$ . In the reversed robustness case, the conjunction ( $\wedge$ ) and the always ( $\square$ ) correspond to the convex function (max) while the disjunction ( $\vee$ ) and the eventually ( $\diamond$ ) operators correspond to concave function (min). It is important to note that this modification does not alter all the properties of the original robustness since we only reverse the signs in the definition of the robustness function as in (8).

#### B. Tree structure

We will now introduce a tree structure for STL formulas, namely a *robustness tree*  $\mathcal{T}^{\varphi}$ , which is defined for the reversed robustness functions  $\rho_{\text{rev}}^{\varphi}$  constructed from Definition 1. While the authors of [8, 15, 26] also define a tree structure of STL formulas, their motivations differ slightly from ours: [8, 15] focus on MIP-based formulations, while [26] concentrates on back-propagation for learning methods. It is worth noting that our tree structure is defined directly to the reversed robustness function, rather than to the formula.

*Definition 2: (Robustness Tree)* A robustness tree  $\mathcal{T}^{\varphi}$  is a tuple  $(\mathcal{O}, \mathcal{A}, \mathcal{S})$  corresponding to reversed robustness function  $\rho_{\text{rev}}^{\varphi}$ , where

- i)  $\mathcal{O} \in \{\max, \min\}$  is the type of the top node of the tree  $\mathcal{T}^{\varphi}$ , which corresponds to the outermost operator of robustness function  $\rho_{\text{rev}}^{\varphi}$ ;
- ii)  $\mathcal{A} = [\mathcal{T}^{\varphi_1}, \mathcal{T}^{\varphi_2}, \dots, \mathcal{T}^{\varphi_N}]$  is a list of  $N$  subtrees (i.e., children) sprouted from the top node, which corresponds to each argument (function) of robustness function  $\rho_{\text{rev}}^{\varphi}$ ;
- iii)  $\mathcal{S} = [t^{\varphi_1}, t^{\varphi_2}, \dots, t^{\varphi_N}]$  is a list of time steps of each subtree.  $t^{\varphi_1}$  and  $t^{\varphi_N}$  correspond to the subscripts of the temporal operator;

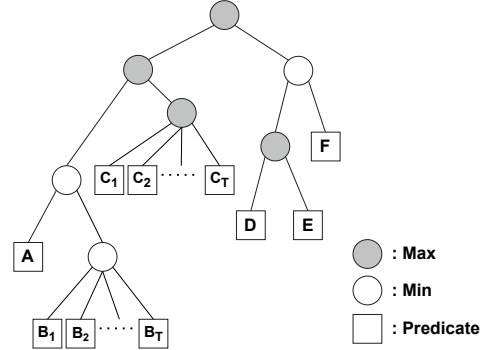


Fig. 1: An example of the robustness tree for formula  $\varphi = ((A \vee \diamond_{[1, T]} B) \wedge \square_{[1, T]} C) \wedge ((D \wedge E) \vee F)$ , where  $A, B, C, D, E, F$  denotes predicates. The grey circles are expressing the max operators, whereas the white circles are expressing the min-type operators. The square boxes are expressing predicates.

Given a robustness function  $\rho_{\text{rev}}^{\varphi}$  (or formula  $\varphi$  itself), the robustness tree  $\mathcal{T}^{\varphi}$  can be built up recursively. An example of the robustness tree is shown in Fig. 1. As we can see, all the bottom nodes of a robustness tree, which we call *leaves*, are predicates. Moreover, all the subtrees in a robustness tree are themselves robustness trees. Thus, every node in a robustness tree is either a max-type node or a min-type node, except for the bottom nodes. As these max-type nodes (resp. the min-type nodes) in the robustness tree correspond to  $\wedge$  and  $\square$  (resp.  $\vee$  and  $\diamond$ ) from Definition 1, they are sometimes referred as conjunctive nodes (resp. disjunctive nodes) depending on the context. In this sense,  $\wedge$  and  $\square$  (resp.  $\vee$  and  $\diamond$ ) are treated similarly. On the other hand, the until operator  $\mathcal{U}$  does not correspond to a single node as it consists of a conjunction of the max and min functions. It corresponds to a tree whose top node is max-type, whose child nodes are min-type nodes, and whose child nodes are min-type nodes or predicates.

For the later discussion, given a robustness tree of  $\mathcal{T}^\varphi$ , we denote the number of nodes whose operator type is min as  $N_V^\varphi$  (which correspond to the disjunctive operators in STL formulas) and denote the number of leaves (predicates) as  $N_p^\varphi$ . Also, we denote the number of leaves whose parent node is max type as  $N_{p\wedge}^\varphi$ , and min type as  $N_{p\vee}^\varphi$  where  $N_p^\varphi = N_{p\wedge}^\varphi + N_{p\vee}^\varphi$  holds.

*Example 1:* Consider the formula in Fig.1, i.e.,  $\varphi = ((A \vee \diamond_{[1,T]} B) \wedge \square_{[1,T]} C) \wedge ((D \wedge E) \vee F)$ . There are three max-type trees (associated with robustness trees  $\mathcal{T}^\varphi$ ,  $\mathcal{T}^{D \vee E}$  and  $\mathcal{T}^{((A \vee \diamond_{[1,T]} B) \wedge \square_{[1,T]} C)}$ ), three min-type trees (associated with robustness trees  $\mathcal{T}^{(A \vee \diamond_{[1,T]} B)}$ ,  $\mathcal{T}^{\diamond_{[1,T]} B}$  and  $\mathcal{T}^{(D \wedge E) \vee F}$ ), and  $2T + 4$  predicates. Hence,  $N_V^\varphi = 3$ ,  $N_p^\varphi = 2T + 4$ . Trees  $\mathcal{T}^\varphi$ ,  $\mathcal{T}^{A \vee \diamond_{[1,T]} B}$ , and  $\mathcal{T}^{\diamond_{[1,T]} B}$  has 2, 2, and  $T$  subtrees respectively and their lists of time steps are  $[0, 0]$ ,  $[0, 0]$ , and  $[0, 1, \dots, T]$  respectively.

### C. Convex-concave procedure (CCP)

The difference of convex (DC) programs constitutes a class of optimization problems for which the convex-concave procedure (CCP) [6, 7] is a heuristic method to find a local optimum. The DC programs can be defined as follows:

*Definition 3: (Difference of convex (DC) programs)*

$$\text{minimize } f_0(\mathbf{z}) - g_0(\mathbf{z}) \quad (9a)$$

$$\text{subject to } f_i(\mathbf{z}) - g_i(\mathbf{z}) \leq 0, \quad i \in \{1, \dots, m\}, \quad (9b)$$

where  $\mathbf{z} \in \mathbb{R}^h$  is the vector of  $h$  optimization variables and the functions  $f_i : \mathbb{R}^h \rightarrow \mathbb{R}$  and  $g_i : \mathbb{R}^h \rightarrow \mathbb{R}$  are convex for  $i \in \{0, \dots, m\}$ . The DC problem (9) can also include equality constraints

$$p_i(\mathbf{z}) = q_i(\mathbf{z}), \quad (10)$$

where  $p_i$  and  $q_i$  are convex. These equality constraints are expressed as the pair of inequality constraints

$$p_i(\mathbf{z}) - q_i(\mathbf{z}) \leq 0, \quad q_i(\mathbf{z}) - p_i(\mathbf{z}) \leq 0. \quad (11)$$

Note that  $f_i(\mathbf{z}), g_i(\mathbf{z})$  can be 0. The class of DC programs is broad; the almost only condition imposed on the program is merely to know whether each function is convex or concave. Thus, once they are known, a wide range of nonconvex programs become DC programs.

The CCP involves a majorization step, where concave terms are replaced with a convex upper bound, and a minimization step, where the resulting convex problem is solved. In this study, we adopt the simplest form of majorization, which is linearization at the current point at each iteration. Specifically, three types of functions in (9) are linearized:

*Definition 4: (Convex-Concave Procedure (CCP))* CCP is an iterative procedure that linearizes all of the following three types of functions at each iteration:

- i) function  $g_0(\mathbf{z})$  in the cost (9a);
- ii) functions  $g_i(\mathbf{z})$  in inequality constraints (9b);
- iii) functions  $p_i(\mathbf{z})$  and  $q_i(\mathbf{z})$  in equality constraints (10),

where all functions are non-affine convex functions. It is worth noting that the third form, non-affine convex functions  $p_i(\mathbf{z})$  and  $q_i(\mathbf{z})$  in equality constraints (10) are also approximated by CCP. This is because an equality constraint

is transformed into two inequalities (11) and both convex functions can make either inequality concave.

The CCP can be shown that (i) all of the iterates are feasible if the starting point is in the feasible set and (ii) the objective value converges (possibly to negative infinity, see [6, 27] for a proof). Thus, it does not need to restrict the update at each iteration (nor to perform a line search), contrary to the traditional SQP methods that often limit the update in the trust regions. Moreover, CCP often converges within fewer iterations than traditional SQP methods.

## IV. ROBUSTNESS DECOMPOSITION

### A. Basic idea of our robustness decomposition

In this section, we present the basic idea of our robustness decomposition. The goal of our decomposition is to turn the problem into a DC program in order to apply a CCP-based algorithm. To this end, we need to know whether each function in the program (6) is convex or concave. In this program (6), the robustness function  $\rho_{\text{rev}}^\varphi$  is the only part whose curvature (convex or concave) cannot be determined. Thus, if the robustness function, which is a composite function consisting of the max and min functions, can be rewritten as a combination of convex and concave functions, the entire program can be reduced to a DC program. The proposed framework achieves this by recursively decomposing the outermost operator of the robustness function using new variables. According to the composition rule in Appendix A, the max and min functions are needed to be decomposed until their arguments become all affine in order to know convex or concave. If the arguments of a function are all predicates, the operator in front of it can be either a max or min function. The recursive decomposition of a nonconvex robustness function into predicates corresponds to a decomposition of the robustness tree from the top to the bottom, in accordance with the tree structure.

The proof of the following theorem shows a naive and elementary procedure for the robustness decomposition using variables, which reformulates Problem 1 into a DC problem.

*Theorem 1:* The program (6) can be equivalently transformed into a difference of convex (DC) program.

*Proof.* We constructively prove the statement. As the robustness function is in the cost function, the first procedure is to decompose the function from the cost function into a set of constraints. We describe the procedure for both cases where the outermost operator of the robustness function  $\rho_{\text{rev}}^\varphi$  is max and min. If the outermost operator is max, i.e.,  $\rho_{\text{rev}}^\varphi = \max(\rho_{\text{rev}}^{\varphi_1}, \rho_{\text{rev}}^{\varphi_2}, \dots, \rho_{\text{rev}}^{\varphi_r})$ , we replace the cost function with variable  $s_\xi$ , and add the constraint

$$\max(\rho_{\text{rev}}^{\varphi_1}, \rho_{\text{rev}}^{\varphi_2}, \dots, \rho_{\text{rev}}^{\varphi_r}) = s_\xi. \quad (12)$$

If the outermost operator is min, i.e.,  $\rho_{\text{rev}}^\varphi = \min(\rho_{\text{rev}}^{\varphi_1}, \rho_{\text{rev}}^{\varphi_2}, \dots, \rho_{\text{rev}}^{\varphi_r})$ , we replace the cost function with variable  $s_\xi$  and add the constraint

$$\min(\rho_{\text{rev}}^{\varphi_1}, \rho_{\text{rev}}^{\varphi_2}, \dots, \rho_{\text{rev}}^{\varphi_r}) = s_\xi. \quad (13)$$

After the first decomposition above, the robustness function in the cost is now decomposed into the constraint of the form,

either (12) or (13). Note that the arguments of both max and min functions in the constraints are still not necessarily predicates. We continue the same kind of replacement until all the arguments in each function become the predicates: for the constraint of max-form (12), we check whether each argument of the max function is a predicate or not. If all these functions are predicates, we do not have to do any additional steps because function  $\varphi$  is determined to be the concave function from the composition rule. However, if not, we cannot decide whether the term is concave or not. Thus, in this case, we replace each argument that is not a predicate,  $\rho_{\text{rev}}^{\varphi_i}$ , with a variable  $s_{\text{new}}$  as  $\max(\rho_{\text{rev}}^{\varphi_1}, \dots, s_{\text{new}}, \dots, \rho_{\text{rev}}^{\varphi_r})$ . Then we add the equality constraint  $\rho_{\text{rev}}^{\varphi_i} = s_{\text{new}}$ , which is of the form either (12) or (13). The procedure for the constraint of min-form (13) is the same as the case of (12) above. After applying these replacements for all the non-predicate arguments, all the new constraints are again of the form either (12) or (13). We repeat this procedure until we reach the predicates, the bottom of the STL tree.

When we finish the above recursive manipulations, all the output constraints are of the form either (12) or (13), and the arguments of all max and min functions become affine. Thus, from the composition rule (Appendix A), the curvature (convex or concave) of max and min functions are known. This concludes the proof.  $\square$

### B. Fewer non-convex parts via recursive epigraphic reformulations

While the naive decomposition method outlined above is easy to understand, it fails to fully leverage the structure of the problem. Specifically, because all new constraints (12) and (13) take the form of *nonaffine equality*, when they are encoded as two inequality constraints as detailed in Subsection III-C, the number of concave constraints needlessly increases. As each step requires more approximations on those concave terms, this would result in either a large number of iterations or an unsatisfactory local solution. Therefore, it is preferable to reduce the non-convex parts of the program to minimize the iterative approximation by the algorithm. To this end, the rest of the section is devoted to introducing a more elaborated reformulation procedure by using the monotonicity property of STL. After introducing this procedure, we show that this reformulation is *equivalent*<sup>2</sup>. Procedure 1 below uses the idea of the epigraphic reformulation methods, which transform the convex (usually linear) cost function into the corresponding epigraph constraints. However, our approach is different from the normal epigraphic reformulation-based approach in the sense that we deal with *nonconvex* cost functions and we have to apply reformulation *recursively*.

**Procedure 1: (Part i. From cost to constraints)** To extract the robustness function from the cost function, the initial step involves decomposing the function into a series of constraints. This process varies depending on whether the outermost

operator of the robustness function  $\rho_{\text{rev}}^{\varphi}$  is a max or min, which is described in **(i. max)** and **(i. min)**, respectively as follows. Note that the max cases are generally simpler than the min cases.

**(i. max)** We first consider the case when the outermost operator of  $\rho_{\text{rev}}^{\varphi}$  is max, i.e.,  $\rho_{\text{rev}}^{\varphi} = \max(\rho_{\text{rev}}^{\varphi_1}, \rho_{\text{rev}}^{\varphi_2}, \dots, \rho_{\text{rev}}^{\varphi_r})$ . In this case, we introduce a new variable  $s_{\xi}$ , and reformulate the program as follows:

$$\min_{\mathbf{x}, \mathbf{u}, s_{\xi}} s_{\xi} \quad (14a)$$

$$\text{s.t. } x_{t+1} = Ax_t + Bu_t \quad (14b)$$

$$x_t \in \mathcal{X}, u_t \in \mathcal{U} \quad (14c)$$

$$s_{\xi} \leq 0 \quad (14d)$$

$$\rho_{\text{rev}}^{\varphi_1}(\mathbf{x}) \leq s_{\xi} \dots \rho_{\text{rev}}^{\varphi_r}(\mathbf{x}) \leq s_{\xi} \quad (14e)$$

**(i. min)** Next, we consider the case when the outermost operator of  $\rho_{\text{rev}}^{\varphi}$  is min, i.e.,  $\rho_{\text{rev}}^{\varphi} = \min(\rho_{\text{rev}}^{\varphi_1}, \rho_{\text{rev}}^{\varphi_2}, \dots, \rho_{\text{rev}}^{\varphi_r})$ . In this case, we first check whether the function  $\varphi_i$  is a predicate or not for all  $i = 1, \dots, r$ . If at least one function  $\varphi_i$  is not a predicate, we next replace  $\rho_{\text{rev}}^{\varphi_i}$  with a variable. This step has to be considered differently depending on whether the outermost operator of  $\rho_{\text{rev}}^{\varphi_i}$  is max or min, as will be explained in **(i. min-max)** and **(i. min-min)**, respectively.

**(i. min-max)** If the outermost operator of function  $\rho_{\text{rev}}^{\varphi_i}$  ( $i = 1, \dots, r$ ) is max, i.e.,  $\rho_{\text{rev}}^{\varphi_i} = \max(\rho_{\text{rev}}^{\phi_1}, \dots, \rho_{\text{rev}}^{\phi_y})$ , we first replace  $\rho_{\text{rev}}^{\varphi_i}$  with a variable  $s$  in  $\rho_{\text{rev}}^{\varphi}$  as  $\min(\rho_{\text{rev}}^{\varphi_1}, \dots, s, \dots, \rho_{\text{rev}}^{\varphi_r})$ , then we add the following constraints:

$$\rho_{\text{rev}}^{\phi_1} \leq s, \dots, \rho_{\text{rev}}^{\phi_y} \leq s. \quad (15)$$

**(i. min-min)** On the other hand, if the outermost operator of the function  $\rho_{\text{rev}}^{\varphi_i}$  ( $i = 1, \dots, r$ ) is min, i.e.,  $\rho_{\text{rev}}^{\varphi_i} = \min(\rho_{\text{rev}}^{\phi_1}, \dots, \rho_{\text{rev}}^{\phi_y})$ , we cannot apply the same transformation above. To replace  $\rho_{\text{rev}}^{\varphi_i}$  with a variable  $s$  in  $\rho_{\text{rev}}^{\varphi}$  as  $\min(\rho_{\text{rev}}^{\varphi_1}, \dots, s, \dots, \rho_{\text{rev}}^{\varphi_r})$ , we need to add non-convex constraints:

$$\min(\rho_{\text{rev}}^{\phi_1}, \dots, \rho_{\text{rev}}^{\phi_y}) = s. \quad (16)$$

**(Part ii. from constraints to constraints)** After these procedures, regardless of the outermost operator of the robustness function, either max or min, the robustness function in the objectives are now decomposed into the constraints in one of the three forms (16), (17), or (18):

$$\max(\rho_{\text{rev}}^{\Phi_1}, \dots, \rho_{\text{rev}}^{\Phi_{y_{\text{max}}}}) \leq s_{\text{max}}, \quad (17)$$

$$\min(\rho_{\text{rev}}^{\Psi_1}, \dots, \rho_{\text{rev}}^{\Psi_{y_{\text{min}}}}) \leq s_{\text{min}}, \quad (18)$$

where  $s_{\text{min}}, s_{\text{max}}$  are variables and each function  $\rho_{\text{rev}}^{\Phi_i}$  ( $i = 1, \dots, y_{\text{max}}$ ),  $\rho_{\text{rev}}^{\Psi_i}$  ( $i = 1, \dots, y_{\text{min}}$ ) is a robustness function associated with subformulas  $\Phi_i$  ( $i = 1, \dots, y_{\text{max}}$ ) and  $\Psi_i$  ( $i = 1, \dots, y_{\text{min}}$ ). These inequalities are paraphrased expressions of (14e) and (15) above. Note that these arguments of the max and min functions are still not necessarily predicates. We continue the following steps until all the arguments in each function become the predicates.

**(ii. max)** For inequality constraints of the form (17), we transform it as follows:

$$\rho_{\text{rev}}^{\Phi_1} \leq s_{\text{max}}, \rho_{\text{rev}}^{\Phi_2} \leq s_{\text{max}}, \dots, \rho_{\text{rev}}^{\Phi_{y_{\text{max}}}} \leq s_{\text{max}}. \quad (19)$$

<sup>2</sup>In the rest of this paper, the term *equivalent* when applied to two optimization problems means that the (global) optimal objective value and optimal solution (if they exist) of one problem can be obtained from those of the other, and vice versa. This is the same usage as in [28, p.257].

This is of course equivalent with (17).

**(ii. min)** For constraints of the forms (16) or (18), we check whether each argument of the min of the left-hand side is a predicate or not, as the explanation of the case **(i. min)**. We then replace arguments that are not a predicate with variables depending on whether the outermost operators of those arguments are max or min, which will be described in **(ii. min-max)** and **(ii. min-min)** respectively. Each procedure is the same as **(i. min-max)** and **(i. min-min)** respectively except for one difference in the following **(ii. min-max)**.

**(ii. min-max)** If the outermost operator of the function  $\rho_{\text{rev}}^{\Psi_i}$  ( $i \in \{1, \dots, y_{\text{min}}\}$ ) is max, i.e.,  $\rho_{\text{rev}}^{\Psi_i} = \max(\rho_{\text{rev}}^{\psi_1}, \dots, \rho_{\text{rev}}^{\psi_v})$ , we first replace function  $\rho_{\text{rev}}^{\Psi_i}$  by a variable  $s_{\text{new}}$  as  $\min(\rho_{\text{rev}}^{\psi_1}, \dots, s_{\text{new}}, \dots, \rho_{\text{rev}}^{\psi_{y_{\text{min}}}})$ . Then, we add the following constraints:

$$\max(\rho_{\text{rev}}^{\psi_1}, \dots, \rho_{\text{rev}}^{\psi_v}) \leq s_{\text{new}}, \quad (20)$$

which is in the same form as (17).

**(ii. min-min)** If the outermost operator of the function  $\rho_{\text{rev}}^{\Psi_i}$  ( $i \in \{1, \dots, y_{\text{min}}\}$ ) is min, i.e.,  $\rho_{\text{rev}}^{\Psi_i} = \min(\rho_{\text{rev}}^{\psi_1}, \dots, \rho_{\text{rev}}^{\psi_v})$ , the procedure is the same as **(i. min-min)**, which produce a new equality constraint of the form (16).

Subsequent to these procedures in **(Part ii.)**, constraints of the form (16), (17), or (18) are decomposed into constraints of one of these same forms. After we repeat this **(Part ii.)** again, these constraints are decomposed into the same forms. We repeat **(Part ii.)** until we reach the predicates, the bottom of the STL tree. This is the end of the procedure.

After this procedure, all concave constraints are in the forms of (16) or (18). The cost function is concave if and only if the outermost operator of the reversed robustness function is min. The other parts of the program are all convex.

### C. Removing min-type equations by formula simplification

Although Procedure 1 remarkably makes the non-affine equality constraints fewer than the procedure described in the proof of Theorem 1, the reformulated program has still a considerable number of equality constraints of the form (16), which have to be approximated by CCP. To address this issue associated with the equations of the form (16), we additionally introduce an offline technique, called the simplification technique [8]. The simplification technique can unify (or remove) max and min functions in succession. This technique was first utilized in [8] for STL specifications to make integer variables fewer in the MIP-based formulation. However, we use this technique to remove the equations of the form (16) for our robustness decomposition. This can be easily explained through the tree structure of a robustness function: if there are two nodes whose type is the same (either max or min), then they can be unified into one node. Note that this unification is applied not only for boolean operators  $\vee, \wedge$  but also temporal operators ( $\square, \diamond, U$ ) as they are expressed as either max or min explained in Subsection III-A. We show an illustrative example of this simplification technique in Fig.2, where the simplified version of the robustness tree in Fig.1 is shown.

We recursively simplify the tree from the top node to the bottom. If there may be more than two consecutive nodes that

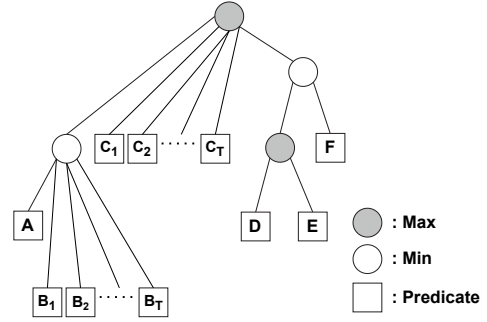


Fig. 2: The simplified version of the robustness tree in Fig.1.

are the same type (e.g. min-min-min...), we repeat this simplification procedure (function SIMPLIFYONCE in Algorithm 4) until it does not have any consecutive same type nodes. As a result, the min-type equations (16) in **(i. min-min)** and **(ii. min-min)** can be removed by executing the simplification offline before the robustness decomposition, resulting in a fewer approximation by CCP at each iteration. Moreover, this simplification brings us another benefit, i.e., it decreases the number of constraints. This is because the order of the constraints' number is proportional to that of nodes' number  $\mathcal{O}(N_{\mathcal{P}}^{\varphi} + N_{\mathcal{V}}^{\varphi})$  where  $N_{\mathcal{V}}^{\varphi}$  decreases when we use the simplification technique. In the rest of this paper, formula  $\varphi$  indicates the simplified formula  $\varphi$  using this simplification technique offline. The overall reformulation procedure in Subsections IV-B and IV-C is summarized in Algorithm 1.

### D. The resulting program and its properties

If the outermost operator (top node) of the robustness function  $\rho_{\text{rev}}^{\varphi}$  is max function, the resulting program  $\mathcal{P}_{\text{DC}}$  is written as follows.

$$\min_{\mathbf{z}} s_{\xi} \quad (21a)$$

$$\text{s.t. } x_{t+1} = Ax_t + Bu_t \quad (21b)$$

$$x_t \in \mathcal{X}, u_t \in \mathcal{U} \quad (21c)$$

$$s_{\xi} \leq 0, \quad (21d)$$

$$\left. \begin{array}{l} \rho_{\text{rev}}^{\Phi_1^{(1)}} \leq s_{\text{max}}^{(1)}, \dots, \rho_{\text{rev}}^{\Phi_{y_{\text{max}}}^{(1)}} \leq s_{\text{max}}^{(1)} \\ \vdots \\ \rho_{\text{rev}}^{\Phi_1^{(v)}} \leq s_{\text{max}}^{(v)}, \dots, \rho_{\text{rev}}^{\Phi_{y_{\text{max}}}^{(v)}} \leq s_{\text{max}}^{(v)} \end{array} \right\} \text{from max nodes} \quad (21e)$$

$$\left. \begin{array}{l} \min(\rho_{\text{rev}}^{\Psi_1^{(1)}}, \dots, \rho_{\text{rev}}^{\Psi_{y_{\text{min}}}^{(1)}}) \leq s_{\text{min}}^{(1)} \\ \vdots \\ \min(\rho_{\text{rev}}^{\Psi_1^{(w)}}, \dots, \rho_{\text{rev}}^{\Psi_{y_{\text{min}}}^{(w)}}) \leq s_{\text{min}}^{(w)} \end{array} \right\} \text{from min nodes} \quad (21f)$$

where  $\mathbf{z} = [\mathbf{x}^{\text{T}}, \mathbf{u}^{\text{T}}, s_{\xi}, s_{\text{max}}^{(1)}, \dots, s_{\text{max}}^{(v)}, s_{\text{min}}^{(1)}, \dots, s_{\text{min}}^{(w)}]^{\text{T}} \in \mathbb{R}^{n+m+1+v+w}$  denotes the vector of optimization variables, where some slight abuse of notation is made such that some of the variables  $s_{\text{max}}^{(v)}, s_{\text{min}}^{(v)}$  in constraints (21e),(21f) may represent  $s_{\xi}$ , and some of the arguments of the min functions (21f) are variables  $s_{\text{max}}^{(v)}$ . Note that all the robustness functions  $\rho_{\text{rev}}^{\varphi}$  in this program are affine predicates and there are no max functions in this program anymore.

---

**Algorithm 1** Program reformulation
 

---

**Input:** Original program (6)

**Output:** The reformulated program (**Cost**, **Constr**)

```

1: Simplify the formula (Algorithm 4);
2: Constr ← {(6b), (6c)}
3: if  $\rho_{\text{rev}}^{\varphi} = \max(\rho_{\text{rev}}^{\varphi_1}, \rho_{\text{rev}}^{\varphi_2}, \dots, \rho_{\text{rev}}^{\varphi_r})$  then
4:   Cost ← {(14a)};
5:   Constr ← Constr  $\cup$  {(14d), (14e)};
6: else (if  $\rho_{\text{rev}}^{\varphi} = \min(\rho_{\text{rev}}^{\varphi_1}, \rho_{\text{rev}}^{\varphi_2}, \dots, \rho_{\text{rev}}^{\varphi_r})$ )
7:   for each  $i \in \{1, \dots, r\}$  do
8:     if  $\rho_{\text{rev}}^{\varphi_i}$  is not a predicate then
9:       replace  $\rho_{\text{rev}}^{\varphi_i}$  in the arguments of  $\rho_{\text{rev}}^{\varphi}$  with a new
       variable  $s_i$ ;
10:    Constr ← Constr  $\cup$   $\{\max(\rho_{\text{rev}}^{\varphi_1}, \dots, \rho_{\text{rev}}^{\varphi_y}) \leq s\}$ ;
11:    Cost ← {(6a)};
12:    Constr ← Constr  $\cup$  {(6d)};
13: while  $\neg(\forall \text{constr} \in \text{Constr}, \text{every argument of the}$ 
    l.h.s of constr is either a predicate or a variable) do
14:   if constr is max form (17) then
15:     for each  $i \in \{1, \dots, y_{\text{max}}\}$  do
16:       if not all the arguments are predicates then
17:         Constr ← Constr  $- \{(17)\}$ ;
18:         Constr ← Constr  $\cup \{(19)\}$ ;
19:       if constr is min form (18) then
20:         for each  $i \in \{1, \dots, v\}$  in (18) do
21:           for each  $i \in \{1, \dots, y_{\text{min}}\}$  do
22:             Constr ← Constr  $- \{(18)\}$ ;
23:             Constr ← Constr  $\cup$   $\{\min(\rho_{\text{rev}}^{\Psi_1}, \dots, s_{\text{new}}, \dots, \rho_{\text{rev}}^{\Psi_{y_{\text{min}}}}) \leq s_{\text{min}}\}$ ;
24:             Constr ← Constr  $\cup \{(20)\}$ ;

```

---

If the outermost operator is min, the resulting program is the same as the program (21), except that the cost function is a min function. However, it is worth noting that most of the specifications are of the max type, which is referred to as conjunction normal form (CNF) in [29], as specifications are typically written as a conjunction of sub-tasks such as reaching goals, avoiding obstacles, and so on. Moreover, the robustness simplification procedure does not change the type of the tree of  $\mathcal{T}^{\varphi}$ . Therefore, in the remainder of this paper, we concentrate on the STL formulas whose robustness tree  $\mathcal{T}^{\varphi}$  is max type for ease of explanation.

We now show that the reformulation by Algorithm 1 does not lose important properties of the original program (6) in the following two theorems. First, this transformation retains the soundness property.

*Theorem 2:* A feasible solution  $\mathbf{x}$  of the program  $\mathcal{P}_{\text{DC}}$  always satisfies the STL specification  $\varphi$ , i.e.,  $\mathbf{x} \models \varphi$ .

*Proof.* From the equations (4) and (8), it is enough to show  $\rho_{\text{rev}}^{\varphi}(\mathbf{x}') \leq 0$ . This equation can be proved in the same way as the proof of [22, Proposition 1]. The only difference is whether we apply the Algorithm 1 for program  $\mathcal{P}_{\text{DC}}$  itself or its smoothed program, which does not affect the proof.  $\square$

The following theorem states that the transformation is *equivalent* in our sense (see footnote 2).

*Theorem 3:* The program  $\mathcal{P}_{\text{DC}}$  is equivalent with (6).

*Proof.* This statement can be proved in the same way as the proof of [22, Theorem 1]. The only difference is whether we

apply Algorithm 1 for program  $\mathcal{P}_{\text{DC}}$  itself or its smoothed program, which does not affect the proof.  $\square$

By these two statements, this reformulation is guaranteed to retain the original properties. Next, the following three propositions state that the resulting program  $\mathcal{P}_{\text{DC}}$  not only takes the DC form, but also has nice properties that can be used to make the CCP framework more efficient. First of all, from (21), we can easily conclude the next fact.

*Proposition 1:* The program  $\mathcal{P}_{\text{DC}}$  does not have nonaffine equality constraints.

Due to this property, we can see from Definition 4 that the parts of the program that we approximate are only inequalities in (21f). Moreover, by inspecting Procedure 1 from the tree perspective, we can see that those concave parts come only from *truly* disjunctive parts (21f) in  $\mathcal{P}_{\text{DC}}$ .

*Proposition 2:* Each concave constraint (21f) of the program  $\mathcal{P}_{\text{DC}}$  corresponds *one-to-one* with a disjunctive node in the simplified robustness tree.

Therefore, we can conclude that the concave parts are minimized and their curvature corresponds to the maximum curvature of each min function. As the convergence of the algorithm is faster in general when the curvature of the concave part is small [16, 17], this property is suitable for our framework. Furthermore, the next fact is stated for Section VI.

*Proposition 3:* The program  $\mathcal{P}_{\text{DC}}$  is a linear program except for the concave constraints of the form (21f).

*Proof.* From (21), we can see that the cost function is a linear function and the constraints are all affine except for inequalities of the form (21f) as we remove all the max functions in the end.  $\square$

## V. SMOOTH APPROXIMATION BY MELLOWMIN

Another advantage of the resulting DC program  $\mathcal{P}_{\text{DC}}$  (21) is that smoothing only a small number of min functions in (21f) makes the program differentiable as other functions are all differentiable. Although we can choose to solve the non-differentiable program (21) directly, this paper focuses on designing gradient-based algorithms. To this end, this section presents a novel min's smooth approximation that is suitable for our framework. Then, we define the corresponding robustness measure.

### A. Alternative smooth approximation

In the literature [3, 4], the max and min functions in the robustness function (7) are smoothed by using the log-sum-exp (LSE) function, which we denote them as  $\overline{\text{max}}_k := \frac{1}{k} \ln \sum_{i=1}^r e^{k a_i}$  and  $\overline{\text{min}}_k := -\overline{\text{max}}_k(-\mathbf{a})$  respectively, where  $k \in \mathbb{R}$  is the smooth parameter. Although this smooth function is differentiable everywhere, the resulting robustness is not sound (4) when we smooth the max and min functions of the robustness function with these  $\overline{\text{max}}_k$  and  $\overline{\text{min}}_k$  functions. This is a serious defect as a measure for guaranteeing safety. To make the smooth approximation sound, we have to smooth the min function with an over-approximation (note that we consider the reversed robustness  $\rho_{\text{rev}}^{\varphi}$ ). With this in mind, we



propose an alternative smooth function for the min function, which we call a mellowmin operator, expressed as follows.

*Definition 5: (Mellowmin operator)*

$$\widetilde{\min}_k(\mathbf{a}) = -\text{mm}_k(-\mathbf{a}), \quad (22)$$

where  $\mathbf{a} = [a_1, \dots, a_r]^\top$  and  $\text{mm}_k(\mathbf{a}) = \frac{1}{k} \ln \left( \frac{1}{r} \sum_{i=1}^r e^{ka_i} \right)$  denotes the mellowmax function.

The mellowmax operator was proposed as an alternative softmax operator in reinforcement learning in [30] and can be thought of as a log-average-exp function, which is an under-approximation of max function. Thus,  $\widetilde{\min}_k$  is an over-approximation of min.

*Lemma 1:* The mellowmin function  $\widetilde{\min}_k$  (22) is an over-approximation of the true min, and its error bound is given by:

$$0 \leq \widetilde{\min}_k(\mathbf{a}) - \min(\mathbf{a}) \leq \frac{\log(r)}{k}. \quad (23)$$

*Proof.* See Appendix B.  $\square$

### B. Our new robustness

Now, we define a new robustness measure using the mellowmin function (22).

*Definition 6: (Reversed mellowmin robustness)* The reversed mellow robustness  $\widetilde{\rho}_{\text{rev}}^\varphi(\mathbf{x})$  is defined by the quantitative semantics of (7) where every min function is replaced by the mellowmin operator  $\widetilde{\min}$  (22).

It is worth mentioning that our new robustness measure considers smooth approximation *only* for the min functions in the robustness (as max functions are rather decomposed).

*Theorem 4: (Soundness)* For any trajectories  $\mathbf{x}$  and any STL specification  $\varphi$ ,  $\widetilde{\rho}_{\text{rev}}^\varphi(\mathbf{x})$  is sound, i.e.,

$$\widetilde{\rho}_{\text{rev}}^\varphi(\mathbf{x}) \leq 0 \implies \mathbf{x} \models \varphi. \quad (24)$$

*Proof.* See Appendix C.  $\square$

*Theorem 5: (Asymptotic completeness)* For any trajectories  $\mathbf{x}$  and any STL specification  $\varphi$ , there exists a constant  $k_{\min} (> 0)$  such that

$$|\rho_{\text{rev}}^\varphi(\mathbf{x}) - \widetilde{\rho}_{\text{rev}}^\varphi(\mathbf{x})| \leq \epsilon \text{ for all } k \geq k_{\min}. \quad (25)$$

*Proof.* See Appendix D.  $\square$

This theorem ensures that the new robustness  $\widetilde{\rho}_{\text{rev}}^\varphi(\mathbf{x})$  approaches the original robustness (3) as  $k$  approaches  $\infty$ , meaning that this robustness asymptotically recovers the completeness property, i.e.,  $\widetilde{\rho}_{\text{rev}}^\varphi(\mathbf{x}) \geq 0 \implies \mathbf{x} \not\models \varphi$ .

Using the smoothed min function above, we restate the program (26) by replacing the robustness (6a) with the new robustness in Definition 6:

$$\min_{\mathbf{x}, \mathbf{u}} \widetilde{\rho}_{\text{rev}}^\varphi(\mathbf{x}) \quad (26a)$$

$$\text{s.t. } x_{t+1} = Ax_t + Bu_t \quad (26b)$$

$$x_t \in \mathcal{X}, u_t \in \mathcal{U} \quad (26c)$$

$$\widetilde{\rho}_{\text{rev}}^\varphi(\mathbf{x}) \leq 0 \quad (26d)$$

Then, Algorithm 1 can transform this program into the program (21) such that min functions in (21f) are replaced by  $\widetilde{\min}$  operators. Let us denote this smoothed program (26) as  $\widetilde{\mathcal{P}}_{\text{DC}}$ .

### C. Advantages of using the mellowmin operator

As we can see in Theorems 4 and 5, the reversed mellow robustness function is sound and asymptotically complete. However, if our goal is to only satisfy these properties, we do not have to use the mellowmin operators. For example, the min functions can also be replaced by the following soft-min operator:

$$\widehat{\min}(\mathbf{a}) := -\frac{\sum_{i=1}^r a_i e^{-ka_i}}{\sum_{i=1}^r e^{-ka_i}}. \quad (27)$$

However, there are three important reasons that we should use the mellowmin operator. First of all, the curvature of the mellowmin is explicit. This is indispensable because the curvature of functions (convex or concave) must be acknowledged to use the CCP-based algorithm.

*Proposition 4:* The mellowmin is concave for any  $k > 0$ .

*Proof.* See Appendix E.  $\square$

On the other hand, the curvature (convex or concave) of the soft-min function (27) cannot be determined as it depends on the parameter  $k$ . Thus, this function cannot be used for our CCP-based approach in the first place. Moreover, the mellowmin is the only function that over-approximates the true min among the functions in Table III in Appendix F, which summarizes the convexity and monotonicity of max, min, and their smooth approximations.

Furthermore, the mellowmin function has also strict monotonicity, which is needed to prove the soundness and the equivalence of the reformulated program in the same way as the proof of Theorems 2 and 3.

*Proposition 5:* The mellowmin is strictly increasing with respect to each of its arguments for all values of the parameter  $k$  s.t.  $0 < k < \infty$ .

*Proof.* See Appendix G.  $\square$

Additionally, the next propositions state that the concaveness of the mellowmin operator is bounded by a value for a given  $k$ , and the bound *gradually* decreases as  $k \rightarrow 0$ .

*Proposition 6:* The mellowmin operator approaches the average operator as  $k$  goes to 0 while it approaches the min operator as  $k$  goes to  $\infty$ , i.e.,

$$\lim_{k \rightarrow \infty} \widetilde{\min}_k(\mathbf{a}) = \min(\mathbf{a}) \quad (28)$$

$$\lim_{k \rightarrow 0} \widetilde{\min}_k(\mathbf{a}) = \text{mean}(\mathbf{a}). \quad (29)$$

*Proof.* See Appendix H.  $\square$

*Proposition 7:* The Hessian of the mellowmin operator is bounded by the following equation:

$$-k \|\mathbf{v}\|^2 \leq \mathbf{v}^\top \nabla^2 \widetilde{\min}_k(\mathbf{a}) \mathbf{v} \leq 0, \quad (30)$$

where  $\mathbf{v} \in \mathbb{R}^r$  and  $\|\mathbf{v}\|^2 = \mathbf{v}^\top \mathbf{v}$ . This bound becomes tighter *monotonically* as  $k \rightarrow 0$ .

*Proof.* See Appendix I.  $\square$

From these propositions and Proposition 2, we can also see that the concaveness (bound) of the overall program  $\widetilde{\mathcal{P}}_{\text{DC}}$  increases *monotonically* as  $k \rightarrow \infty$ . In other words, the

program (26) gets closer to the original program (6) as  $k \rightarrow \infty$  whereas it becomes a *convex* program as  $k \rightarrow 0$ .<sup>3</sup> This property is useful in our framework as we can see the trade-off between the roughness of the majorization at each step and the completeness (see Theorem 2), which can be controlled by the parameter  $k$ . Due to these three reasons, the mellowmin function is the most suitable for CCP among the functions presented in Table III.

## VI. ITERATIVE OPTIMIZATION WITH PENALTY CCP

### A. Properties of the subproblem

After we obtain the resulting program  $\tilde{\mathcal{P}}_{DC}$ , we apply an algorithm based on CCP. In general, the subprogram becomes a general convex program such as second-order cone programs (SOCP) and we have to solve them sequentially. This heavy computational burden is a potential drawback of the CCP-based algorithm. However, in the proposed method, the subproblem we solve at each iteration is a linear (or quadratic) program while retaining all the information of the convex parts.

*Theorem 6:* The program  $\tilde{\mathcal{P}}_{DC}$  after the majorization of CCP in Definition 4 is a linear program (LP). If we add the quadratic cost function, the program can be written as a convex quadratic program (QP).

*Proof.* Proposition 3 implies that the statement holds for (21), where the concave parts in (21f) are linearized during the majorization step.  $\square$

As a corollary of the above theorem, our CCP-based method is sequential linear programming. If we add the quadratic cost function in (26a), our method becomes sequential quadratic programming (SQP). Let  $\mathcal{P}_{LP}$  denote the linear subproblem.

Furthermore, regardless of this computational efficiency above, the number of concave constraints (21f) is relatively small compared to the total number of constraints, as demonstrated by the following theorem and example.

*Theorem 7:* The CCP in Definition 4 only linearizes the constraints of the form (21f) whose number is proportional to the number of disjunctive nodes  $N_{\vee}^{\varphi}$  in the STL formulas, i.e.,  $\mathcal{O}(N_{\vee}^{\varphi})$  whereas the number of all the constraints is proportional to the number of  $N_{p\wedge}^{\varphi}$ ,  $N_{\vee}^{\varphi}$ , and  $T$ , i.e.,  $\mathcal{O}(N_{p\wedge}^{\varphi} + N_{\vee}^{\varphi} + T)$ .

*Proof.* As the program does not have non-affine equality constraints as in Proposition 1, concave constraints are only of the form (21f). Proposition 2 states that these concave parts correspond to the disjunctive nodes of simplified robustness tree  $\mathcal{T}^{\varphi}$ . On the other hand,  $\mathcal{O}(N_{p\wedge}^{\varphi})$  comes from (21e), and  $\mathcal{O}(T)$  comes from (21b) and (21c).  $\square$

*Example 2:* Consider the formula in Example 1 with  $T = 20$ . The number of concave constraints is 2, while the number of convex (including affine) constraints is 83, where 22 comes

<sup>3</sup>This is because, if all min functions become average functions, the robustness becomes a convex function. The authors of [12] leverage this property to make the program a convex quadratic program. However, they had to restrict the range of STL specifications considerably. In this sense, our work can be seen as the extension of their work, where we allow all the STL specifications.

from equations in (21e), and 61 comes from equations in (21b), (21c), and (21d).

Furthermore, the feasible solution of the resulting program  $\mathcal{P}_{LP}$  also has soundness property.

*Theorem 8:* Let a decision variable vector  $\mathbf{z} = [\mathbf{x}^T, \dots]^T$  be a feasible solution to the program  $\mathcal{P}_{LP}$ . The feasible trajectory  $\mathbf{x}$  always satisfies the STL specification  $\varphi$ , i.e.,  $\mathbf{x} \models \varphi$ .

*Proof.* See Appendix J.  $\square$

### B. Tree-weighted penalty CCP

In this subsection, we propose a heuristic extension of CCP, which we call the *tree-weighted penalty CCP (TWP-CCP)*, to improve the algorithm further by exploiting the *hierarchical* information of STL. Generally speaking, in an STL specification, each logical operator does not have the same importance. Using the words of the STL tree, nodes whose subtree has more leaves (predicates) are more essential than nodes whose subtree has fewer leaves because the precision of the former has a higher influence on the overall tree than that of the latter. Therefore, we give the priority ranking among nodes in proportion to the number of leaves they have. This priority information should be taken into account, particularly in the early stages of the optimization process. Otherwise, there is a possibility that the *important* constraints will be considerably violated in the early stages, leading subsequent steps to go in the wrong direction.

To add this priority information into the algorithm, we follow the idea of *penalty CCP* [6], where the constraint relaxation was introduced to remove the need for an initial feasible point to start the algorithm. They relax the problem by adding variables to the constraints and penalizing the sum of the violations by adding them to the objective function. We extend this idea by leveraging the fact in Proposition 2 that, in the resulting program, each constraint corresponds to an operator in the simplified STL specification individually. This property can be used to penalize the violation differently. We impose the priority weights on the penalty variable in each constraint where the weights are proportional to the number of leaves that the corresponding node has. For instance, the relaxed program of (9) is as follows:

$$\min_{\mathbf{z}} f_0(\mathbf{z}) - g_0(\mathbf{z}) + \tau_i \sum_{j=1}^m N^{\varphi_j} s_j \quad (31a)$$

$$\text{s.t. } f_j(\mathbf{z}) - g_j(\mathbf{z}) \leq s_j, j = 1, \dots, m \quad (31b)$$

$$s_j \geq 0, j = 1, \dots, m. \quad (31c)$$

The TWP-CCP procedure is summarized in Algorithm 2, where  $\mathbf{z}_{(i)}$  denotes the current value at each iteration. The meaning of other symbols is the same as Subsection III-C.

As the program (31) reduces to program  $\mathcal{P}_{LP}$  when  $s_j \rightarrow 0$  for  $j \in \{1, \dots, m\}$  ( $\tau_i \rightarrow \infty$ ), the solution obtained from program  $\mathcal{P}_{LP}$  satisfies the STL specification in this limit. Moreover, the soundness property holds even when the introduced relaxation variables  $s_j$  do not take the value 0, by adjusting the threshold, which can be calculated using the monotonicity property.

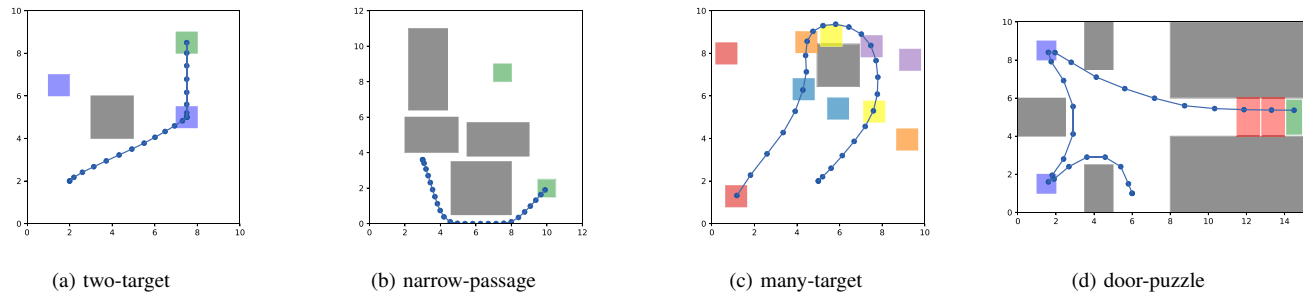


Fig. 3: Illustrations of scenarios along with solutions generated by MIP-based method with  $T = 25$ .

---

### Algorithm 2 Tree-Weighted Penalty CCP

---

**Input:** Parameters: an initial point  $z_0$ , an initial weight  $\tau_0 > 0$  and its maximum constant  $\tau_{\max} > 0$  and its rate of change at each iteration,  $\mu > 1$ , and a stopping criterion.

- 1: Compute the number of leaves  $N^{\varphi_j}$  associated with each constraint for  $j = 1, \dots, m$ , and initialize:  $i := 0$ ;
  - 2: Majorize the concave terms  $g_j, j = 0, \dots, m$  in (31) to  $\hat{g}_j(z) = g_j(z_{(i)}) + \nabla g_j(z_{(i)})^\top (z - z_{(i)})$  and solve the convex program;
  - 3: Update  $\tau_{i+1} := \min(\mu\tau_i, \tau_{\max})$ ;
  - 4: Update iteration as  $i := i + 1$ . Repeat until the stopping criterion is satisfied;
- 

*Theorem 9:* We consider the program  $\mathcal{P}_{\text{DC}}$  whose  $w$  concave constraints (21f) are relaxed with the variables  $s_j (j = 0, \dots, w)$  as (31) and other constraints are not relaxed. Let the stopping criterion be  $\max_j(s_j) \leq s_c$  where  $s_c$  is a constant. Then, Any feasible solution that satisfies this stopping criterion also satisfies the STL specification  $\varphi$  by changing the threshold of the constraints (21d) from 0 to  $-ws_c$ , i.e.,  $s_\xi < -ws_c$ .

*Proof.* See Appendix K.  $\square$

In practice, the resulting values of the penalty variables are very close to 0 if it converges, and thus, we do not have to care about the thresholds.

To our knowledge, this is the first framework that utilizes the *priority* information of STL operators for optimization algorithms. Although some papers have viewed STL as a tree, this priority ranking among nodes has been missed in the literature. This was because there was no connection between constraints and nodes of the STL tree in the original formulation. In contrast, we establish a connection between them by the reformulation. The overall framework *STLCCP* is summarized in Algorithm 3.

---

### Algorithm 3 STLCCP

---

- 1: Transform Problem 1 to (26) by applying new smooth robustness in Definition 6 (Sections III and V);
  - 2: Reformulate (26) into  $\tilde{\mathcal{P}}_{\text{DC}}$  (e.g. (21)) by Algorithm 1 (Section IV);
  - 3: Optimize via tree-weighted penalty CCP by Algorithm 2 (Section VI);
- 

## VII. NUMERICAL EXPERIMENTS

In this section, we demonstrate the effectiveness of our proposed method over state-of-the-art methods through four benchmark scenarios. During the experiment in Subsection VII-F, we also propose a practical remedy, the warm-start approach, to effectively utilize the mellowmin functions. All experiments were conducted on a MacBook Air 2020 with an Apple M1 processor (Maximum CPU clock rate: 3.2 GHz) and 8GB of RAM. Note that in this section, all robustness scores refer to the scores calculated from the original robustness semantics (3).

### A. Compared methods

**Proposed Algorithm:** We implemented our algorithm in Python using CVXPY [31] as the interface to the optimizer. As for the smooth min function for reversed robustness function, the first three experiments in VII-C–VII-E focus on the LSE smoothing ( $k = 10$ ) in [22, Definition 2] to show the validity of our reformulation method, whereas the final subsection shows the effectiveness of the mellowmin smoothing ( $k = 1000$ ) in Definition 6. For the solving step, we used the QP-solver of GUROBI (ver. 10) [32] with the default option (parallel barrier algorithm). We took the TWP-CCP described in Subsection III-C to solve the reformulated program unless otherwise noted. The penalty variables were introduced only for the concave constraints as in Theorem 9. This is because CCP only approximates such concave parts and there is less need to admit the violation for the convex parts. We employed a normal distribution to vary the initial values of variables in each sample. If the optimization failed to converge within 25 iterations, we regarded our method as unsuccessful and terminated the optimization. However, in most of the problems we solved, the terminal condition was met within 15 iterations. All the parameters for the CCP shown in Table IV in Appendix L are fixed throughout this paper.

The compared two methods are summarized as follows. They are one of the most popular and fastest methods in MIP-based and the SQP-based method, respectively.

**MIP-based approach: GUROBI-MIP** For the MIP-based approach, we formulated the problem as a MIP one using the encoding framework in [33] and solved the problem with the GUROBI solver, which we call GUROBI-MIP method. Note that GUROBI is often the fastest MIP solver.

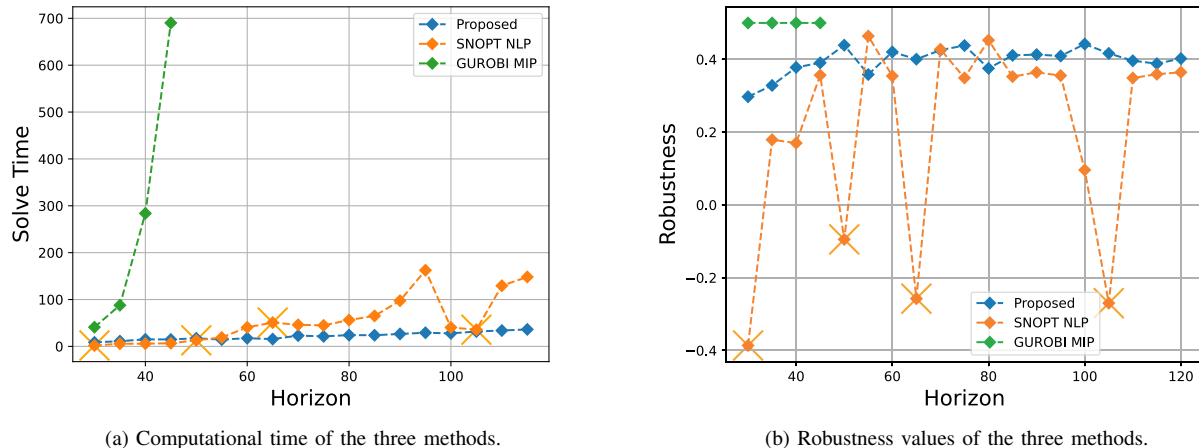


Fig. 4: Computational time and robustness score of the three methods in the many-target scenario over Horizon from  $T = 30$  to 120.

**SQP-based approach: SNOPT-NLP** The SQP-based method we employed is based on the naive sequential quadratic programming (SQP) approach using the smoothing method proposed in [5] where they combine smoothing method using LSE and Boltzman softmax. Among the various SQP-based solvers available, we chose the SNOPT sparse SQP solver [34] because it is considered to be one of the best solvers for STL specifications among the SQP approaches, which outperforms Scipy’s SQP solver (similar arguments can be found in [5, 8]). All the parameter options of the SNOPT-NLP method were left at their default settings. We refer to this method as the SNOPT-NLP method.

### B. Systems and specifications

Note that the state  $\mathbf{x}$  and input  $\mathbf{u}$  are defined as  $\mathbf{x} = [p_x, p_y, \dot{p}_x, \dot{p}_y]^\top$   $\mathbf{u} = [\ddot{p}_x, \ddot{p}_y]^\top$ , where  $p_x$  is the horizontal position of the robot and  $p_y$  is the vertical position. As for the system dynamics, we use a double integrator, i.e., a system (1) with the matrices

$$A = \begin{bmatrix} I_2 & I_2 \\ 0_{2 \times 2} & I_2 \end{bmatrix}, \quad B = \begin{bmatrix} 0_{2 \times 2} \\ I_2 \end{bmatrix}. \quad (32)$$

All four benchmark scenarios were borrowed from [8], which are standard scenarios involving a robot exploring a planar environment. The illustration of all four scenarios above is shown in Figures 3c, with the solution obtained by MIP based method with  $T = 25$ . In this picture, the greyed regions express obstacles ( $O$ ) that the robot must avoid for all time steps. The green regions express goals ( $G$ ) that the robot must reach at the last time step. Other regions colored purple, blue and orange, and pink represent areas that the robot must pass through (or stop by) at least one-time step. For the specification of two-target and narrow-passage, the robot must pass through one of the two same color regions, while in the many-target specification, the robot must reach both two same color regions. In the door-puzzle specification, the robot has to collect keys ( $K$ ) in the two blue regions to open the corresponding doors represented by the red and green

regions in the figure. Specifically, the STL specification for each scenario is expressed as the following four formulas.

#### two-target:

$$\diamond_{[0, T-5]} (\square_{[0, 5]} T_1 \vee \square_{[0, 5]} T_2) \wedge \square_{[0, T]} \neg O \wedge \diamond_{[0, T]} G \quad (33a)$$

#### narrow-passage:

$$\diamond_{[0, T]} (G_1 \vee G_2) \wedge \square_{[0, T]} \left( \bigwedge_{i=1}^4 \neg O_i \right) \quad (33b)$$

#### many-target:

$$\bigwedge_{i=1}^5 \left( \bigvee_{j=1}^2 \diamond_{[0, T]} T_i^j \right) \wedge \square_{[0, T]} (\neg O), \quad (33c)$$

#### door-puzzle:

$$\bigwedge_{i=1}^2 (\neg D_i \mathbf{U}_{[0, T]} K_i) \wedge \diamond_{[0, T]} G \wedge \square_{[0, T]} \left( \bigwedge_{i=1}^5 \neg O_i \right). \quad (33d)$$

We would like to insist that the robot is not given the value of the initial speed in all the scenarios. Let us choose a specification from equations of (33) and express it as  $\varphi$ . We provide four sets of experimental results, each corresponding to each subsection.

*Remark 3: (Small quadratic cost)* To show our framework is effective in practical situations, we introduced a quadratic cost function  $w_q \sum_{t=0}^T (x_t^\top Q x_t + u_t^\top R u_t)$ , where  $Q$  and  $R$  are positive semidefinite symmetric matrices and  $w_q$  is a weight parameter. The value of  $w_q$  was set to 0.01 or 0.001.

*Remark 4: (A modification for the SNOPT-NLP)* In almost all the scenarios, the SNOPT-NLP solver returns the infeasible error message for the problem we consider. To make the comparison more meaningful, we removed the robustness constraint (6d) from Problem 1 only when we use the SNOPT-NLP method, which makes the problem easier to solve for the method.

### C. Comparison over different horizons

As the first experiment, we evaluated the performance of our proposed method against the SQP-based method and the

TABLE II: Solve times and robustness scores for the four different scenarios. Each value for our method represents the average of successful trials out of 10. If the robustness score for the SNOPT-NLP method is negative, it is labeled as “Failed”. If the solve time for GUROBI-MIP exceeds the allotted time of 7500, it is labeled as “Time out”.

Scenario	Horizon (T)	Solve Time (s)		
		Ours	SNOPT-NLP	MIP
two-target	50	23.13	<b>15.28</b>	15.08
	75	<b>26.76</b>	Failed	193.82
	100	<b>37.19</b>	57.24	337.31
many-target	50	<b>16.19</b>	Failed	2526.99
	75	<b>21.45</b>	44.78	>7500.00
	100	<b>27.80</b>	40.39	>7500.00
narrow-passage	50	<b>22.21</b>	Failed	36.74
	75	65.65	<b>8.83</b>	>7500.00
	100	57.41	<b>39.94</b>	>7500.00
door-puzzle	50	<b>299.33</b>	Failed	>7500.00
	75	Failed	Failed	>7500.00
	100	Failed	Failed	>7500.00

(a) Computational time

Scenario	Horizon (T)	Robustness		
		Ours	SNOPT-NLP	MIP
two-target	50	<b>0.494</b>	0.367	0.500
	75	<b>0.500</b>	Failed	0.500
	100	<b>0.500</b>	0.462	0.500
many-target	50	<b>0.440</b>	Failed	0.500
	75	<b>0.430</b>	0.349	Time Out
	100	<b>0.437</b>	0.096	Time Out
narrow-passage	50	<b>0.151</b>	Failed	0.400
	75	0.027	<b>0.151</b>	Time Out
	100	0.111	<b>0.170</b>	Time Out
door-puzzle	50	<b>0.348</b>	Failed	Time Out
	75	Failed	Failed	Time Out
	100	Failed	Failed	Time Out

(b) Robustness Score

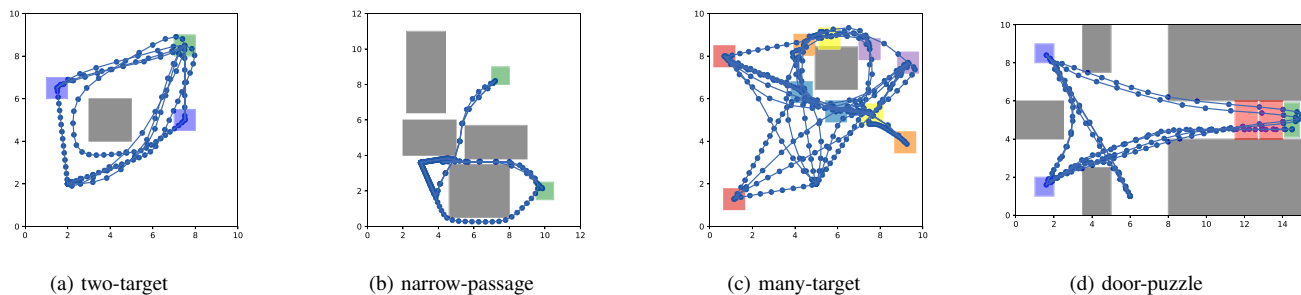


Fig. 5: Illustrations of scenarios along with the satisfactory trajectories generated by the proposed method with  $T = 50$ . Our method produced a range of satisfactory trajectories, each dependent on the initial guesses.

MIP-based method on a specific scenario, that is, the many-target specification (33c), with varying time horizons ranging from  $T = 30$  to 120. The results are presented in Fig. 4, which compares the computation time of the three methods in Fig. 4a and their corresponding robustness scores in Fig. 4b. Note that in Fig. 4b, the SNOPT-NLP method sometimes takes negative values as we omit the robustness constraint (6d) for this method (see Remark 4). The orange  $\times$  marker in Fig. 4a shows the SNOPT-NLP’s failure at the corresponding time horizon, meaning that the SNOPT-NLP method is stuck to local solutions with robustness less than or equal to 0, as shown in Fig. 4a. The blue plots in these figures are representing the average values of 5 trials of the proposed method as these results significantly depend on the initial value of variables. We omit the box plot of the variance for the sake of visibility (the variance is plotted in the box plot of Fig. 6). In the case of the other two methods, on the other hand, the results do not change by trial.

The computation time of the MIP-based method increases significantly as the horizon increases. The comparison of the two SQP-based methods shows that our proposed method was able to find satisfactory trajectories for all horizons within the given range of horizons, whereas the SQP-based method failed to find solutions on four horizons of  $T = 30, 50, 65,$  and  $105$  (marked by the orange  $\times$ ). It is worth noting that the robustness scores of our proposed method were consistently higher than 0, not only in the average of 5 samples but also in each of the five samples. This means that our method was

successful in 95 out of 95 ( $19 \times 5$ ) experiments (100.00 %). On the other hand, the SNOPT-NLP method succeeds in 15 out of 19 samples (78.95 %) even though the robustness constraint (26d) is turned off.

Moreover, the convergence time of our proposed method only increases *slightly* as the horizon increases. In contrast, the SNOPT-NLP method experiences significant fluctuations in its performance as the horizon gets larger, and it takes longer to converge than our proposed method for all horizons  $T \geq 55$ , with a poorer robustness value in most cases. It’s worth noting that while the computation time of the SNOPT-NLP method may appear to decrease at horizons  $T = 100, 105$ , this is due to either a failure ( $T = 105$ ) or a low robustness value of approximately 0.1 ( $T = 100$ ), as shown in Fig. 4b, indicating that the optimization process is getting stuck in a local solution at an early stage of the optimization. Fig. 4b also demonstrates that our proposed method consistently takes a higher robustness score than the SNOPT-NLP method, achieving an average score of around 0.4, which is close to the global optimum 0.5 obtained by the MIP-based method. In contrast, the SNOPT-NLP method outputs a failure trajectory with a negative robustness value in some horizons.

Our method’s superiority in this scenario can be attributed to the fact that the number of concave constraints (21f) (81) is significantly less than the total number of constraints in (21) (3579 including all the constraints in (21b)–(21f)).

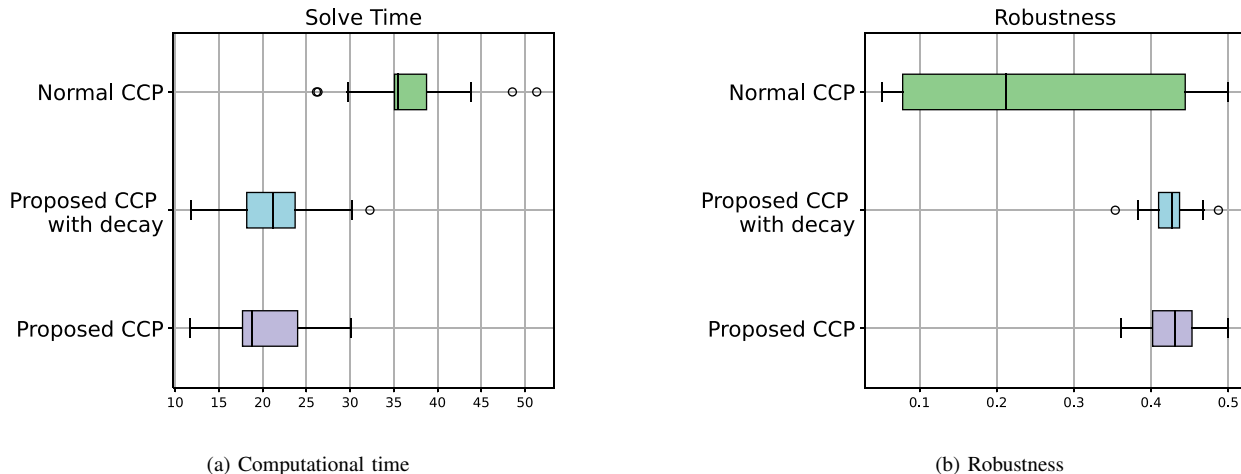


Fig. 6: Box plots of 20 samples for each method concerning computational time and robustness value for the many-target scenario with  $T = 75$ .

#### D. Comparison over different specifications

Our next experiment compared the performance of three methods across four different scenarios, namely the two-target, narrow-passage, many-target, and door-puzzle scenarios. Table IIa presents the convergence times of the three methods, and Table IIb shows their corresponding robustness scores. They essentially show that only our method can output satisfactory trajectories for all the horizons of the two-target, many-target, and narrow-passage scenarios. Moreover, our method significantly outperforms the other methods in both the two-target and many-target specifications. Furthermore, Only our method is able to synthesize a satisfactory trajectory for the door-puzzle scenario with  $T = 50$ .

It should be noted that the success rate of our method was above 90% in the two-target (27/30) and narrow-passage scenarios (28/30) and 100% in the many-target scenario (30/30), meaning that our method is robust against the initial guesses of variables, whereas, in the door-puzzle scenario, it was 30% (3/10). However, this is remarkable because these difficult scenarios over horizons were thought to be difficult to solve. Although our method also sometimes succeeded in  $T = 75$  and  $T = 100$ , we did not list the details of these cases as their success rates were low.

Table IIa shows that our proposed method is fastest in the majority of the horizons in two-target and many-target scenarios whereas the SNOPT-NLP sometimes does better than our approach in the narrow-passage scenario. Moreover, our method’s convergence time only increases slightly even when the horizon becomes longer, which is consistent with our observations in Subsection VII-C. Table IIb shows that our proposed method consistently produces a range of satisfactory trajectories while the SNOPT-NLP method exhibits a high degree of volatility, with a tendency to fail randomly in certain scenarios. For example, it produced a robustness score of 0.462 out of 0.500 in the two-target specifications with  $T = 100$ , but failed the same specification with  $T = 75$  with a score of  $-0.506$ . On the other hand, each trial of our method has a success rate of almost 100%, not only the averages of 10

trials given different initial values. These results demonstrate that our proposed method is robust against the values of initial guesses.

Fig. 5a–5d displays several final trajectories generated by our proposed method with different initial values for all scenarios with  $T = 50$ . These figures illustrate that our method is flexible enough to find a solution that satisfies the specifications regardless of the initial values.

#### E. Effectiveness of the tree weighted penalty CCP

In the third experiment, we compare the proposed tree-weighted penalty CCP (TWP-CCP) with the standard penalty CCP, referred to as a normal CCP, to show that the TWP-CCP improves the robustness score and convergence time. To make the comparison more persuasive, we also consider a variant of tree-weighted penalty CCP, which we call a proposed CCP with decay, as a comparison method. This method can be considered an intermediary approach between the proposed CCP and the normal CCP. Specifically, this method initially starts as a proposed CCP, which gives priority ranking to the constraints according to the robustness tree, but then it exponentially approaches the normal CCP (see Appendix M for the technical detail).

We evaluate the performance of three different methods in the many-target scenario with horizon  $T = 75$ . The robustness scores and convergence times for each method are illustrated in Figs. 6b and 6a, respectively, using box plots. Each box plot represents the results from 20 samples, which were generated by randomly varying the initial values of the variables.

Fig. 6b shows that the two TWP-CCP methods output much higher robustness scores than the normal CCP, and their convergence times are also lower on average. The results of the proposed method with decay, which only puts tree weight at early iterations, are comparable to the proposed method in Fig. 6b and Fig. 6a. This result suggests a hypothesis that it is essential to incorporate the priority ranking, particularly in the early steps of the optimization process. This hypothesis was also verified when we analyzed how the value of each

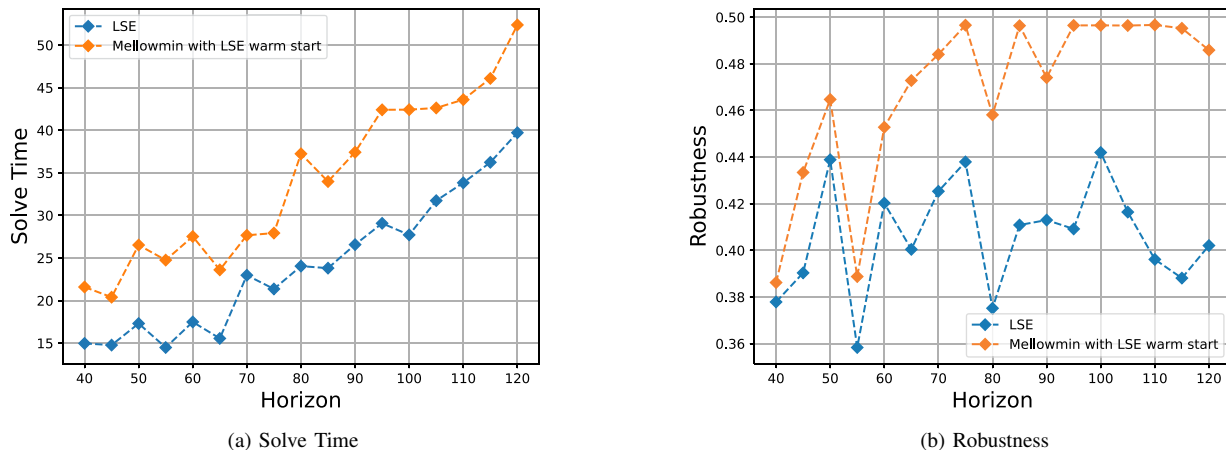


Fig. 7: Computational time and robustness score of the two methods in the many-target scenario over Horizon from  $T = 40$  to 120. The orange plot additionally solves the mellowmin smoothed program  $\tilde{\mathcal{P}}_{DC}$  using the solution of the blue plots (which solves  $\mathcal{P}_{DC}$  smoothed by LSE smoothing).

variable changes during the optimization of the normal CCP. Our experiment shows that when the normal CCP failed to find a satisfactory trajectory, the reason for this failure is, in most cases, high values of variables attached to the important constraints. As they weigh all constraints as equally important, they can easily neglect to observe those constraints, which can lead the optimization process to a local optimum.

#### F. Effectiveness of the mellowmin smoothing

In all experiments in Subsections VII-C–VII-E, we adopted LSE smoothing with  $k = 10$  to demonstrate the effectiveness of our basic idea. However, the LSE smoothing approach does not have the same desirable properties as the mellowmin smoothing approach, such as the soundness property as described in Subsection V-C. Thus, we prefer to solve the mellowmin smoothed program  $\tilde{\mathcal{P}}_{DC}$  in the end. However, we often obtain a poorer solution when solving the mellowmin smoothed program alone. This is likely because the smooth parameter  $k$  of mellowmin must be set high (e.g. 1000) to accurately approximate the true min function, while  $k = 10$  is sufficient for the LSE smoothing case. However, this high value of  $k$  may make the function more likely to be affected by only one argument with the critical value, similar to the true min function, resulting in the transformed program being more prone to getting stuck in a local minimum. Therefore, we propose using the solution obtained from LSE smoothing as a warm start for the mellowmin smoothed program. The following two sets of experimental results demonstrate that this approach brings us a higher robustness score while maintaining theoretical guarantees such as soundness.

Fig. 7 compares the LSE smoothing and mellowmin smoothing using the LSE solution as a warm start in the many-target specification. The difference between the two plots in Fig. 7a represents the time required to solve the mellowmin smoothed program as the additional step. We can observe that the robustness score becomes higher than when solely using the LSE function, which sometimes achieves the global

optimum 0.5. Additionally, the average computational time to solve the mellowmin smoothed program remains low, around 10 seconds, even as the planning horizon increases. This is likely due to the fact that a solution from the LSE smoothed program is often a good trajectory. Moreover, it’s important to note that the resulting solution of the warm start approach is always guaranteed to be sound, i.e.,  $x \models \varphi$ .

We have also validated the effectiveness of this warm-start approach in the door-puzzle scenario. As discussed in Subsection VII-D, while our method was able to generate a satisfactory trajectory using the LSE smoothing approach, we observed an increase in success rate when we repeated the warm-started mellowmin approach (for further details, please refer to the data provided in the GitHub link).

## VIII. CONCLUSION

In this study, we established a connection between STL and CCP, and used it to propose an efficient optimization framework. Our novel structure-aware decomposition of STL formulas enabled us to encode the control problem into an efficient DC program, where only the concave constraints corresponding to the disjunctive nodes of the STL tree were linearized. To further enhance the efficiency and formality of our algorithm, we introduced a new smoothing function, called the mellowmin function, and an extension of CCP, called TWP-CCP. Both of these enhancements were shown to be effective in our experiments.

In future work, we plan to extend our framework to multi-agent systems and explore its applicability to various other problems beyond the trajectory synthesis problem addressed in this study. As our framework is designed to handle any STL specifications, we believe it has broad applicability to a wide range of problems.

## REFERENCES

- [1] O. Maler and D. Nickovic, “Monitoring temporal properties of continuous signals,” in *Formal Techniques, Modelling and Analysis of Timed and Fault-Tolerant Systems*, 2004, pp. 152–166.

- [2] G. E. Fainekos and G. J. Pappas, “Robustness of temporal logic specifications for continuous-time signals,” *Theoretical Computer Science*, vol. 410, no. 42, pp. 4262–4291, 2009.
- [3] Y. V. Pant, H. Abbas, and R. Mangharam, “Smooth operator: Control using the smooth robustness of temporal logic,” in *IEEE Conference on Control Technology and Applications (CCTA)*, 2017, pp. 1235–1240.
- [4] W. Hashimoto, K. Hashimoto, and S. Takai, “STL2vec: Signal temporal logic embeddings for control synthesis with recurrent neural networks,” *IEEE Robotics and Automation Letters*, vol. 7, no. 2, pp. 5246–5253, 2022.
- [5] Y. Gilpin, V. Kurtz, and H. Lin, “A smooth robustness measure of signal temporal logic for symbolic control,” *IEEE Control Systems Letters*, vol. 5, no. 1, pp. 241–246, 2021.
- [6] T. Lipp and S. Boyd, “Variations and extension of the convex–concave procedure,” *Optimization and Engineering*, vol. 17, no. 2, pp. 263–287, 2016.
- [7] X. Shen, S. Diamond, Y. Gu, and S. Boyd, “Disciplined convex–concave programming,” in *IEEE Conference on Decision and Control (CDC)*, 2016, pp. 1009–1014.
- [8] V. Kurtz and H. Lin, “Mixed-integer programming for signal temporal logic with fewer binary variables,” *IEEE Control Systems Letters*, vol. 6, pp. 2635–2640, 2022. Their source code is available at <https://stlpy.readthedocs.io>.
- [9] S. Karaman and E. Frazzoli, “Vehicle routing problem with metric temporal logic specifications,” in *IEEE Conference on Decision and Control (CDC)*, 2008, pp. 3953–3958.
- [10] S. Karaman, R. G. Sanfelice, and E. Frazzoli, “Optimal control of mixed logical dynamical systems with linear temporal logic specifications,” in *IEEE Conference on Decision and Control (CDC)*, 2008, pp. 2117–2122.
- [11] V. Raman, A. Donzé, M. Maasoumy, R. M. Murray, A. Sangiovanni-Vincentelli, and S. A. Seshia, “Model predictive control with signal temporal logic specifications,” in *IEEE Conference on Decision and Control (CDC)*, 2014, pp. 81–87.
- [12] L. Lindemann and D. V. Dimarogonas, “Robust control for signal temporal logic specifications using discrete average space robustness,” *Automatica*, vol. 101, pp. 377–387, 2019.
- [13] N. Mehdipour, C. I. Vasile, and C. Belta, “Specifying user preferences using weighted signal temporal logic,” *IEEE Control Systems Letters*, vol. 5, no. 6, pp. 2006–2011, 2021.
- [14] I. Haghghi, N. Mehdipour, E. Bartocci, and C. Belta, “Control from signal temporal logic specifications with smooth cumulative quantitative semantics,” in *IEEE Conference on Decision and Control (CDC)*, 2019, pp. 4361–4366.
- [15] D. Sun, J. Chen, S. Mitra, and C. Fan, “Multi-agent motion planning from signal temporal logic specifications,” *IEEE Robotics and Automation Letters*, 2022.
- [16] F. Debrouwere, W. Van Loock, G. Pipeleers, Q. T. Dinh, M. Diehl, J. De Schutter, and J. Swevers, “Time-optimal path following for robots with convex–concave constraints using sequential convex programming,” *IEEE Transactions on Robotics*, vol. 29, no. 6, pp. 1485–1495, 2013.
- [17] Q. Tran Dinh, S. Gumussoy, W. Michiels, and M. Diehl, “Combining convex–concave decompositions and linearization approaches for solving BMIs, with application to static output feedback,” *IEEE Transactions on Automatic Control*, vol. 57, no. 6, pp. 1377–1390, 2012.
- [18] M. Cubuktepe, N. Jansen, S. Junges, J.-P. Katoen, and U. Topcu, “Convex optimization for parameter synthesis in MDPs,” *IEEE Transactions on Automatic Control*, vol. 67, pp. 6333–6348, 2021.
- [19] Q. Wang, M. Chen, B. Xue, N. Zhan, and J.-P. Katoen, “Encoding inductive invariants as barrier certificates: Synthesis via difference-of-convex programming,” *Information and Computation*, vol. 289, p. 104965, 2022.
- [20] M. Charitidou and D. V. Dimarogonas, “Signal temporal logic task decomposition via convex optimization,” *IEEE Control Systems Letters*, vol. 6, pp. 1238–1243, 2022.
- [21] Y. Mao, B. Acikmese, P.-L. Garoche, and A. Chapoutot, “Successive convexification for optimal control with signal temporal logic specifications,” in *ACM International Conference on Hybrid Systems: Computation and Control (HSCC)*, 2022, pp. 1–7.
- [22] Y. Takayama, K. Hashimoto, and T. Ohtsuka, “Signal temporal logic meets convex–concave programming: A structure-exploiting SQP algorithm for STL specifications,” *submitted for the proceedings of the IEEE Conference on Decision and Control (CDC)*, Available at <https://arxiv.org/abs/2304.01475>.
- [23] S. Sadraddini and C. Belta, “Formal synthesis of control strategies for positive monotone systems,” *IEEE Transactions on Automatic Control*, vol. 64, no. 2, pp. 480–495, 2019.
- [24] —, “Robust temporal logic model predictive control,” in *Annual Allerton Conference on Communication, Control, and Computing (Allerton)*, pp. 772–779, 2015.
- [25] C. Baier and J.-P. Katoen, *Principles of Model Checking*. MIT Press, 2008.
- [26] K. Leung, N. Aréchiga, and M. Pavone, “Backpropagation for parametric STL,” in *IEEE Intelligent Vehicles Symposium (IV)*, pp. 185–192, 2019.
- [27] B. K. Sriperumbudur and G. R. G. Lanckriet, “On the convergence of the concave–convex procedure,” in *Advances in Neural Information Processing Systems (NIPS)*, vol. 22, 2009.
- [28] G. C. Calafiore and L. El Ghaoui, *Optimization Models*. Cambridge University Press, 2014.
- [29] S. Sadraddini, J. Rudan, and C. Belta, “Formal synthesis of distributed optimal traffic control policies,” in *8th International Conference on Cyber-Physical Systems (ICCPs)*, p. 15–24, 2017.
- [30] K. Asadi and M. L. Littman, “An alternative softmax operator for reinforcement learning,” in *International Conference on Machine Learning (ICML)*, vol. 70, pp. 243–252, 2017.
- [31] S. Diamond and S. Boyd, “CVXPY: A Python-Embedded modeling language for convex optimization,” *Journal of Machine Learning Research*, vol. 17, 2016.
- [32] Gurobi Optimization, LLC, “Gurobi Optimizer Reference Manual,” 2023. [Online]. Available: <https://www.gurobi.com>
- [33] C. Belta and S. Sadraddini, “Formal methods for control synthesis: An optimization perspective,” *Annual Review of Control, Robotics, and Autonomous Systems*, vol. 2, no. 1, pp. 115–140, 2019.
- [34] P. E. Gill, W. Murray, and M. A. Saunders, “SNOPT: An SQP algorithm for large-scale constrained optimization,” *SIAM Review*, vol. 47, pp. 99–131, 2005.
- [35] S. Boyd and L. Vandenberghe, *Convex Optimization*. Cambridge University Press, 2004.
- [36] S. Kim, K. Asadi, M. Littman, and G. Konidaris, “Deepmellow: Removing the need for a target network in deep Q-learning,” in *International Joint Conference on Artificial Intelligence*, 2019, pp. 2733–2739.
- [37] B. Gao and L. Pavel, “On the properties of the softmax function with application in game theory and reinforcement learning,” *arXiv:1704.00805*, 2017.

## APPENDIX

### A. Composition rule [35]

A composition of functions  $f(g_1(z), \dots, g_p(z))$ , where  $f: \mathbb{R} \rightarrow \mathbb{R}$  is convex and  $g_1, \dots, g_p: \mathbb{R}^q \rightarrow \mathbb{R}$ , is convex when it satisfies the following composition rule. Let  $\tilde{f}: \mathbb{R} \rightarrow \mathbb{R} \cup \{\infty\}$  be the extended-value extension of  $f$ . One of the following conditions must be met for each  $i = 1, \dots, p$ :

- i)  $g_i$  is convex and  $\tilde{f}$  is nondecreasing in argument  $i$ .
- ii)  $g_i$  is concave and  $\tilde{f}$  is nonincreasing in argument  $i$ .
- iii)  $g_i$  is affine.

The composition rule for concave functions is analogous.

### B. Proof of Lemma 1

$$\text{mm}_k(\mathbf{a}) - \max(\mathbf{a}) = \frac{-\log(r) + \log(\sum_{i=1}^r e^{k(a_i - \max(\mathbf{a}))})}{k}. \quad (34)$$

Note that  $1 \leq W \leq r$  where  $W$  is defined as  $W := |\{a_i = \max(\mathbf{a}) : i \in \{1, \dots, r\}\}|$ . We consider (34) for the case of the equality conditions of this inequality. When  $W = r$ , i.e.,  $a_1 = a_2 = \dots = a_r$ , the left-hand side of equation (34) is equal to 0, which is the greatest value that the left-hand side can take because of the monotonicity of the log-sum-exp function as in Appendix F. Thus, we get  $\text{mm}_k(\mathbf{a}) - \max(\mathbf{a}) \leq 0$ . By taking a minus sign for the whole expression and a minus sign in front of each argument, we get  $-\text{mm}_k(-\mathbf{a}) + \max(-\mathbf{a}) \geq 0$ , that is,  $\widetilde{\text{min}}_k(\mathbf{a}) - \min(\mathbf{a}) \geq 0$ . Hence, the mellowmin function is an over-approximation of the true min.



On the other hand, when  $W = 1$ , the left-hand side of (34) is greater than  $-\log(r)$ , which is the bound we get, because of the monotonicity of the log-sum-exp. That is,  $\text{mm}_k(\mathbf{a}) - \max(\mathbf{a}) \geq -\log(r)$ . By taking a minus sign for the whole expression and a minus sign in front of each argument, we get inequality (23).

### C. Proof of Theorem 4

From Lemma 1, for any STL formula  $\varphi$  in negation normal form (NNF),

- $\rho_{\text{rev}}^\pi((\mathbf{x}, t)) = \widetilde{\rho}_{\text{rev}}^\pi((\mathbf{x}, t))$
- $\widetilde{\rho}_{\text{rev}}^{\varphi_1 \wedge \varphi_2}((\mathbf{x}, t)) = \rho_{\text{rev}}^{\varphi_1 \wedge \varphi_2}((\mathbf{x}, t))$
- $\widetilde{\rho}_{\text{rev}}^{\varphi_1 \vee \varphi_2}((\mathbf{x}, t)) \geq \rho_{\text{rev}}^{\varphi_1 \vee \varphi_2}((\mathbf{x}, t))$
- $\widetilde{\rho}_{\text{rev}}^{\varphi_1 \square_{[t_1, t_2]} \varphi_2}((\mathbf{x}, t)) = \rho_{\text{rev}}^{\varphi_1 \square_{[t_1, t_2]} \varphi_2}((\mathbf{x}, t))$
- $\widetilde{\rho}_{\text{rev}}^{\varphi_1 \diamond_{[t_1, t_2]} \varphi_2}((\mathbf{x}, t)) \geq \rho_{\text{rev}}^{\varphi_1 \diamond_{[t_1, t_2]} \varphi_2}((\mathbf{x}, t))$
- $\widetilde{\rho}_{\text{rev}}^{\varphi_1 \mathbf{U}_{[t_1, t_2]} \varphi_2}((\mathbf{x}, t)) \geq \rho_{\text{rev}}^{\varphi_1 \mathbf{U}_{[t_1, t_2]} \varphi_2}((\mathbf{x}, t))$ .

By induction, these inequalities follow that

$$\widetilde{\rho}_{\text{rev}}^\varphi(\mathbf{x}) \leq 0 \implies \rho_{\text{rev}}^\varphi(\mathbf{x}) \leq 0 \quad (35)$$

From this relation and (4), equation (24) follows.

### D. Proof of Theorem 5

Recall from Lemma 1 that for  $k \geq \frac{\log(r)}{\epsilon}$ , we have

$$|\min(\mathbf{a}) - \widetilde{\min}(\mathbf{a})| \leq \epsilon. \quad (36)$$

By applying this inequality to the definition of  $\widetilde{\rho}_{\text{rev}}^\varphi$  (7), we have

- $|\widetilde{\rho}_{\text{rev}}^\pi((\mathbf{x}, t)) - \rho_{\text{rev}}^\pi((\mathbf{x}, t))| = 0$
- $|\widetilde{\rho}_{\text{rev}}^{\varphi_1 \wedge \varphi_2}((\mathbf{x}, t)) - \rho_{\text{rev}}^{\varphi_1 \wedge \varphi_2}((\mathbf{x}, t))| \leq 0$
- $|\widetilde{\rho}_{\text{rev}}^{\varphi_1 \vee \varphi_2}((\mathbf{x}, t)) - \rho_{\text{rev}}^{\varphi_1 \vee \varphi_2}((\mathbf{x}, t))| \leq \epsilon$
- $|\widetilde{\rho}_{\text{rev}}^{\varphi_1 \square_{[t_1, t_2]} \varphi_2}((\mathbf{x}, t)) - \rho_{\text{rev}}^{\varphi_1 \square_{[t_1, t_2]} \varphi_2}((\mathbf{x}, t))| \leq 0$
- $|\widetilde{\rho}_{\text{rev}}^{\varphi_1 \diamond_{[t_1, t_2]} \varphi_2}((\mathbf{x}, t)) - \rho_{\text{rev}}^{\varphi_1 \diamond_{[t_1, t_2]} \varphi_2}((\mathbf{x}, t))| \leq \epsilon$
- $|\widetilde{\rho}_{\text{rev}}^{\varphi_1 \mathbf{U}_{[t_1, t_2]} \varphi_2}((\mathbf{x}, t)) - \rho_{\text{rev}}^{\varphi_1 \mathbf{U}_{[t_1, t_2]} \varphi_2}((\mathbf{x}, t))| \leq \epsilon$ .

By induction, inequality (25) holds. A similar proof can be found in [5, 13].

### E. Proof of Proposition 4

As [35, p. 88] and [36, Claim 1], the *mellowmax* function has the analytic form of Hessian:

$$\nabla^2 \widetilde{\max}_k(\mathbf{a}) = \frac{k}{(\mathbf{1}^\top \boldsymbol{\sigma})^2} ((\mathbf{1}^\top \boldsymbol{\sigma}) \text{diag}(\boldsymbol{\sigma}) - \boldsymbol{\sigma} \boldsymbol{\sigma}^\top) \geq 0 \quad (37)$$

where  $\boldsymbol{\sigma} = [\sigma_1, \dots, \sigma_r]^\top$ ,  $\sigma_i = e^{ka_i}$ . Thus, this mellowmax function is convex when the parameter  $k \geq 0$ . By taking a minus sign for the whole expression and a minus sign in front of each argument, we get the Hessian of the mellowmin:  $\nabla^2 \widetilde{\min}_k = -\frac{k}{(\mathbf{1}^\top (-\boldsymbol{\sigma}))^2} ((\mathbf{1}^\top (-\boldsymbol{\sigma})) \text{diag}(-\boldsymbol{\sigma}) - (-\boldsymbol{\sigma})(-\boldsymbol{\sigma})^\top) \leq 0$ . Thus, the mellowmin function (22) is concave as long as  $k \geq 0$ .

### F. Properties of max, min, and their smoothed functions

Convexity, monotonicity, and which approximation (over-approximation or under-approximation) of max, min, and their smoothed functions are summarized as follows.

- i) The max function is a nondecreasing convex function whereas its smooth approximations, i.e., the  $\widetilde{\max}_k$  and function is a strictly increasing convex function.
- ii) The min operator is a nonincreasing convex function whereas its smooth approximations, i.e.,  $\widetilde{\min}_k$  function is a strictly decreasing concave function.

TABLE III: Summary of each function's curvature and which approximation (over-approximation or under-approximation) is used when the parameter  $0 < k < \infty$ . Other smooth max functions are analogous.

function	curvature	approximation
max	convex	–
min	concave	–
$\widetilde{\min}_k$	concave	under-approx. of min
$\widehat{\min}_k$	concave	over-approx. of min
$\widehat{\min}_k$	–	over-approx. of min

### G. Proof of Proposition 5

The derivative of the mellowmin is given as

$$\frac{\partial \widetilde{\min}_k(\mathbf{a})}{\partial a_i} = -\frac{e^{-ka_i}}{\sum_{i=1}^r e^{-ka_i}}, \quad (38)$$

When  $0 < k < \infty$  this is less than 0, i.e.,  $\frac{\partial \widetilde{\min}_k(\mathbf{a})}{\partial a_i} < 0$  [28].

### H. Proof of Proposition 6

As [30, Subsection 5.2], from (34), we get

$$\lim_{\omega \rightarrow \infty} \text{mm}_k(\mathbf{a}) = \max(\mathbf{a}) + \lim_{\omega \rightarrow \infty} \frac{-\log(r) + \log(W)}{k} \\ \therefore \lim_{k \rightarrow \infty} \text{mm}_k(\mathbf{a}) = \max(\mathbf{a}). \quad (39)$$

On the other hand, by [30, Subsection 5.4] using L'Hôpital's rule, we get  $\lim_{k \rightarrow 0} \text{mm}_k(\mathbf{a}) = \text{mean}(\mathbf{a})$ . By taking a minus sign for the whole expression and a minus sign in front of each argument in this equation and (39), we get (28) and (29).

### I. Proof of Proposition 7 [37]

From (37), for all  $a, v \in \mathbb{R}^n$ ,

$$v^\top \nabla^2 \widetilde{\max}_k(\mathbf{a}) v \leq k \sum_{i=1}^n v_i^2 \sigma_i \leq k \sup\{\sigma_i\} \sum_{i=1}^n v_i^2 \quad (40)$$

$$\therefore v^\top \nabla^2 \widetilde{\max}_k(\mathbf{a}) v \leq k \|v\|^2. \quad (41)$$

where  $\sup\{\sigma_i\} = 1, \forall i \in \{1, \dots, n\}, \forall a \in \mathbb{R}^n$ . By taking a minus sign for the whole expression and a minus sign in front of each argument of (37) and this equation, we have the equation (30).

### J. Proof of Theorem 8

The next lemma can be obtained from a CCP's property.

**Lemma 2:** A feasible solution of the linear program  $\mathcal{P}_{LP}$  is a feasible solution to the program  $\tilde{\mathcal{P}}_{DC}$ .

*Proof.* This is because the first-order approximations of CCP at each step are global over-estimators; i.e.,  $f_i(\mathbf{z}) - g_i(\mathbf{z}) \leq f_i(\mathbf{z}) - g_i(\mathbf{z}_{(\cdot)}) + \nabla g_i(\mathbf{z}_{(\cdot)})^\top (\mathbf{z}_{(\cdot)} - \mathbf{z})$  where  $g_i$  is  $\mathbf{z}_{(\cdot)}$  is the current point of variable  $\mathbf{z}$ .  $\square$

On the other hand, we can prove in the same way as Theorem 2 that a feasible solution of the program  $\tilde{\mathcal{P}}_{DC}$  always satisfies  $\tilde{\rho}_{rev}^\varphi(\mathbf{x}') \leq 0$ . From this equation and Theorem 4, this feasible solution  $\mathbf{x}$  always satisfies the specification. Therefore, with Lemma 2 above, the statement holds.

### K. Proof of Theorem 9

The difference between  $\tilde{\mathcal{P}}_{DC}$  and its relaxed program is the terms  $\tau_i \sum_{j=1}^m N^{\varphi_j} s_j$  on the cost (21a) and  $s_j$  for the concave constraints of the form (21f). In the same way as the proof of [22, Proposition 1], we first prove, using the fact that  $\min$  is a strictly increasing function, that inequality

$$\widetilde{\min}(\tilde{\rho}_{rev}^{\Psi_1}, \dots, \tilde{\rho}_{rev}^{\Psi_i}, \dots, \tilde{\rho}_{rev}^{\Psi_{y_{\min}}}) - s_j \leq s_\xi$$

holds, where  $j \in \{1, \dots, w\}$  is the index for  $w$  concave constraints. Similar analogies can be used for all subsequent transformations that follow the same pattern. Therefore,  $\tilde{\rho}_{rev}^\varphi(\mathbf{x}) - ws_c \leq s_\xi$  holds.

Therefore, if we change the threshold in (21d) from 0 to  $-ws_c$  as  $s_\xi < -ws_c$ , then  $\tilde{\rho}_{rev}^\varphi(\mathbf{x}) \leq 0$  holds. From Theorem 4, the statement holds.

### L. Parameter setting in the numerical experiments

TABLE IV: Parameters for CCP.

Parameters	Description	Value
$\tau$	initial weight on penalty variables in the cost	5e-3
$\mu$	rate at which $\tau$ increases	2.0
$\tau_{\max, \mu}$	maximum $\tau$	1e3
$s_{\text{terminal}}$	maximum values of penalty variables for terminal condition	1e-5
$ep$	maximum cost difference for terminal condition	1e-2
$r$	rate of exponential decay (only for Subsection VII-E)	0.2

### M. Detailed settings for two compared methods

The normal CCP and the proposed method with decay can be expressed as follows, where usages of symbols are the same as in Algorithm 2.

**Proposed method with decay:** Let the current iteration number be  $i$ , the tree weight for constraint  $j \in \{1, \dots, m\}$  be  $\min_{j \in J}(N^{\varphi_j})$ , and  $s_j$  be the sum of all the variables of each concave constraint. The proposed CCP with decay adds the following penalty cost for each constraint  $j \in \{1, \dots, m\}$  of the form:

$$\sum_{j=1}^m (N^{\varphi_j} - \min_{j \in J}(N^{\varphi_j}) \exp(-r(i-1)) + \min_{j \in J}(N^{\varphi_j})) \tau s_j \quad (42)$$

where  $r$  is the parameter that adjusts the exponential decay rate.  $\min_{j \in J}(N^{\varphi_j})$  is the lowest number of the tree weight constant. For example, in the case of the many-target scenario with  $T = 75$ , this is 4.

**Normal CCP method:** The normal CCP is the penalty CCP in Algorithm 2 where the penalty weights  $N^{\varphi_j}$  of all the concave constraints  $i \in I$  are equal to the smallest number of child nodes each node has.

### N. The simplification algorithm [8]

---

#### Algorithm 4 simplification( $\mathcal{T}^\varphi$ )

---

**Input:** robustness tree  $\mathcal{T}^\varphi = (\mathcal{O}, \mathcal{A}, \mathcal{S})$

**Output:** Simplified robustness tree

```

1: Flag = True
2: while Flag do
3:   Flag = SIMPLIFYONCE( $\varphi$ )
4: function SIMPLIFYONCE( $\Phi$ )
5:   Flag=false
6:   for each  $i$  in  $\{1, \dots, n\}$  do
7:     if subtree  $\mathcal{T}^{\Phi_i}$  is not a predicate then
8:       if  $\mathcal{O}^\Phi = \mathcal{O}^{\Phi_i}$  then
9:          $\mathcal{A}^\Phi$ .pop( $i$ ) (removes  $i$ -th tree  $\mathcal{T}^{\Phi_i}$ )
10:         $\mathcal{S}^\Phi$ .pop( $i$ ) (removes  $i$ -th timestep  $t^{\Phi_i}$ )
11:         $\mathcal{A}^\Phi \leftarrow \mathcal{A}^\Phi \parallel \mathcal{A}^{\Phi_i}$ 
12:         $\mathcal{S}^\Phi \leftarrow \mathcal{S}^{\Phi_i} + t^{\Phi_i}$  (elementwise plus  $t^{\Phi_i}$ )
13:         $\mathcal{S}^\Phi \leftarrow \mathcal{S}^\Phi \parallel \mathcal{S}^{\Phi_i}$ 
14:        Flag=True
15:   Flag = Flag  $\vee$  SIMPLIFYONCE( $\mathcal{T}^{\Phi_i}$ )
16: Return Flag

```

---